Medicine
Computational and Systems Biology

Multi-tissue network analysis reveals the effect of JNK inhibition on dietary sucrose-induced metabolic dysfunction in rats

Reviewed Preprint
v2 • January 30, 2025
Revised by authors

Reviewed Preprint
v1 • September 12, 2024

Hong Yang, Cheng Zhang, Woonghee Kim, Mengnan Shi, Metin Kilicliogl u, Cemil Bayram, Ismail Bolat, Özlem Özdemir Tozlu, Cem Baba, Nursena Yuksel, Serkan Yildirim, Shazia Iqbal, Jihad Sebhaoui, Ahmet Hacımuftuoglu, Mathias Uhlen, Jan Boren, Hasan Turkez, Adil Mardinoglu

Science for Life Laboratory, KTH - Royal Institute of Technology, Stockholm, Sweden • Department of Pathology, Veterinary Faculty, Atatürk University, Erzurum, Turkiye • Department of Medical Pharmacology, Faculty of Medicine, Atatürk University, Erzurum, Turkiye • Department of Molecular Biology and Genetics, Faculty of Science, Erzurum Technical University, Erzurum, Turkiye • Trustlife Labs Drug Research & Development Center, Istanbul, Turkiye • Department of Molecular and Clinical Medicine, University of Gothenburg, Sahlgrenska University Hospital, Gothenburg, Sweden • Department of Medical Biology, Faculty of Medicine, Atatürk University, Erzurum, Turkiye • Centre for Host-Microbiome Interactions, Faculty of Dentistry, Oral & Craniofacial Sciences, King's College London, London, United Kingdom

eLife Assessment

The authors implement a **valuable** multi-tissue approach to dissect the physiologic consequences of JNK inhibition in parallel with dietary perturbation via sucrose. The conclusions of disrupted liver, muscle and adipose metabolism being central to these effects are **solid**, as they are supported by a combination of experimental dissection and network modeling approaches.

https://doi.org/10.7554/eLife.98427.2.sa3

Abstract

Excessive consumption of sucrose, in the form of sugar-sweetened beverages, has been implicated in the pathogenesis of metabolic dysfunctionLassociated fatty liver disease (MAFLD) and other related metabolic syndromes. The c-Jun N-terminal kinase (JNK) pathway plays a crucial role in response to dietary stressors, and it was demonstrated that the inhibition of the JNK pathway could potentially be used in the treatment of MAFLD. However, the intricate mechanisms underlying these interventions remain incompletely understood given their multifaceted effects across multiple tissues. In this study, we challenged rats with sucrose-sweetened water and investigated the potential effects of JNK inhibition by employing network analysis based on the transcriptome profiling obtained from hepatic and extrahepatic tissues, including visceral white adipose tissue, skeletal muscle, and brain. Our data demonstrate that JNK inhibition by JNK-IN-5A effectively reduces the circulating

triglyceride accumulation and inflammation in rats subjected to sucrose consumption. Coexpression analysis and genome-scale metabolic modelling reveal that sucrose overconsumption primarily induces transcriptional dysfunction related to fatty acid and oxidative metabolism in the liver and adipose tissues, which are largely rectified after JNK inhibition at a clinically relevant dose. Skeletal muscle exhibited minimal transcriptional changes to sucrose overconsumption but underwent substantial metabolic adaptation following the JNK inhibition. Overall, our data provides novel insights into the molecular basis by which JNK inhibition exerts its metabolic effect in the metabolically active tissues. Furthermore, our findings underpin the critical role of extrahepatic metabolism in the development of diet-induced steatosis, offering valuable guidance for future studies focused on JNK-targeting for effective treatment of MAFLD.

Introduction

Hepatic steatosis (HS) is characterized by the accumulation of triglycerides (TG) in the liver (at least 5% of liver weight) in the absence of secondary contributing factors (Nassir et al., 2015). Metabolic dysfunctionLassociated fatty liver disease (MAFLD) encompasses a spectrum of conditions, ranging from simple HS to metabolic dysfunction-associated steatohepatitis (MASH), which is characterized by HS combined with various degrees of liver inflammation and liver injury, with or without fibrosis. MASH can progress to advanced liver disease including cirrhosis and hepatocellular carcinoma (Machado and Cortez-Pinto, 2023). The global prevalence of MAFLD is estimated to be 20~25% (Younossi et al., 2023), and it is rapidly increasing in parallel with the epidemic of obesity and type 2 diabetes mellitus (Kotsiliti, 2023; Le et al., 2023). Given the absence of approved pharmacological therapy for MAFLD by the US Food and Drug Treatment (FDA) (Llovet et al., 2023; Nassir et al., 2015), the discovery and development of effective therapies are of great importance in MAFLD treatment.

The progression of MAFLD is associated with various factors, including overnutrition, genetic determinants, and associated comorbidities (Sveinbjornsson et al., 2022; Yki-Jarvinen et al., 2021). Strong evidence from meta-analysis, prospective cohort studies, and observational studies indicate that excessive sucrose, a disaccharide that comprises equal amounts of glucose and fructose and is prevalent in all kinds of sugar-sweetened beverages, maybe an initial factor for the development of MAFLD (Geidl-Flueck et al., 2021; Geurtsen et al., 2021; Karlsen et al., 2022; Malik and Hu, 2022; Zhang et al., 2021). For instance, a previous study reported that rats subjected to a 12-week high-sucrose diet (25% w/v sucrose), developed a metabolic syndrome phenotype characterized by glucose intolerance, HS, and insulin resistance (IR) (Sousa et al., 2018). Recent research further reveals that the consumption of sucrose at a concentration of 10% w/v can disrupt energy balance and induce HS within 10-20 weeks (Jang et al., 2020; Stephenson et al., 2022). In this context, c-Jun-N-terminal Kinase (JNK), a mitogen-activated protein kinase family member, emerges as a critical player due to its known function in response to intra- and extracellular stress, including hypercaloric diet consumption (Nikolic et al., 2020; Sabio et al., 2009; Softic et al., 2020). Indeed, accumulating evidence implicated JNK in the pathogenesis of diet-induced obesity, IR, development of metabolic syndrome and MAFLD (Czaja, 2010; Sabio and Davis, 2010; Seki et al., 2012; Singh et al., 2009). JNK has three isoforms: JNK1 and JNK2, which are ubiquitously expressed, and JNK3 is specifically expressed in the brain, testis and heart (Chang and Karin, 2001). Previously, Singh et al. demonstrated that increased hepatic JNK signalling occurred simultaneously with steatosis and lipid accumulation in a steatohepatitis model induced by a methionine- and choline-deficient diet (MCD) (Singh et al., 2009). Notably, MCD diet-fed JNK1 null mice exhibited significantly reduced levels of key hallmarks of MAFLD, including HS, TG accumulation, inflammation, lipid peroxidation, hepatocyte injury, and apoptosis (Singh et al., 2009). Similarly, high-fat diet-fed mice with hepatic ablation of both JNK1 and JNK2 are protected from HS and IR (Vernia et al., 2014). Altogether, these findings suggest that the suppression of the JNK pathway may prevent the development of HS and

related metabolic syndrome (Kodama and Brenner, 2009; Schattenberg et al., 2006). However, whether JNK mediates the metabolic disruption induced by sucrose overconsumption remains to be elucidated. Moreover, our previous study demonstrated that JNK-IN-5A, a selective JNK2 and JNK3 inhibitor (Angell et al., 2007; Cerbone et al., 2012), effectively decreased fat accumulation and steatosis-related protein expression in an *in vitro* steatosis model (Kim et al., 2023). However, the inhibitory effect of JNK-IN-5A to JNK and JNK-related pathways in *in vivo* is unknown. It is established that JNK exerts its metabolic regulation as a result of multi-tissue communication, including those between liver and adipose tissues (Azzu et al., 2020), and skeletal muscle (Nikolic et al., 2020; Vernia et al., 2014). A systematic investigation into tissue-specific and tissue-crosstalk metabolic changes in response to diet and therapy interventions is, therefore, paramount by using genome-scale metabolic models (GEMs). GEMs are the collection of biochemical reactions and the associated enzymes and transporters between the cellular compartments and such models can be used in the analysis of omics data for gaining insights and interpretation of the omics data (Mardinoglu et al., 2013; Mardinoglu et al., 2018; Mardinoglu and Nielsen, 2012; Mardinoglu and Palsson, 2024).

In this study, we first performed a 7-day oral toxicology study and studied the tolerability of JNK-IN-5A in rats. Next, we explored the potential therapeutic effect of JNK-IN-5A under high sucrose consumption in *in vivo* by performing systems biology analysis. To elucidate the systems-wide impact of sucrose overconsumption and JNK-IN-5A treatment, we investigated the intra- and inter-tissue response through integrative analysis of transcriptomics profiles from the metabolically active tissues, including liver and three other extrahepatic tissues: visceral white adipose tissue (vWAT), skeletal muscle (SkM), and brain tissues. We further predicted the genome-wide metabolic activity changes induced by liquid sucrose ingestion and JNK-IN-5A treatment by performing genome-scale metabolic modelling.

Results

The acute effect of the JNK-IN-5A in rats

We previously showed that the JNK-IN-5A can effectively decrease the TG accumulation and steatosis-related protein levels in an *in vitro* model simulating the activated *de novo* lipogenesis in MAFLD patients (Kim et al., 2023). Here, we first performed a 7-day oral toxicology study and studied the tolerability of JNK-IN-5A in rats. Four groups of three males and three females were given vehicle and doses of 30, 100 and 300 mg/kg of JNK-IN-5A, once a day for 7 days (**Fig. 1**, **Fig. 2a**). We assessed clinical adverse effects, body weight, and clinical pathological parameters during the study.

A few animals including those given vehicles displayed noisy respiration and reflux. These signs were only observed in connection with dosing, suggesting being related to the high viscosity of the formulation and foul taste, and are not considered as systemic side effects of the JNK-IN-5A administration. We observed none of the administrated doses led to significant changes in body weight and haematological parameters (**Data S1**). Clinical chemistry parameters revealed lower plasma levels of glucose, blood urea nitrogen and total proteins in female rats given JNK-IN-5A at all three doses (**Fig. 2a**, **Data S1**). In addition, the two higher doses of JNK-IN-5A decreased the levels of sodium in female rats and elevated the level of phosphate in both sexes (**Fig. 2a**, **Data S1**). Overall, the administration of JNK-IN-5A is well tolerated with regard to adverse clinical signs, body weight and clinical haematology parameters.

Treatment of liquid sucrose-induced fatty liver with JNK-IN-5A

We next investigated the effect of JNK-IN-5A treatment in a rat model of MAFLD induced by liquid sucrose ingestion (**Fig. 1b**). The rats feeding a standard chow diet received either tap water (control group) or sucrose-containing water (10% w/v sucrose, sucrose group) for 4 weeks, after

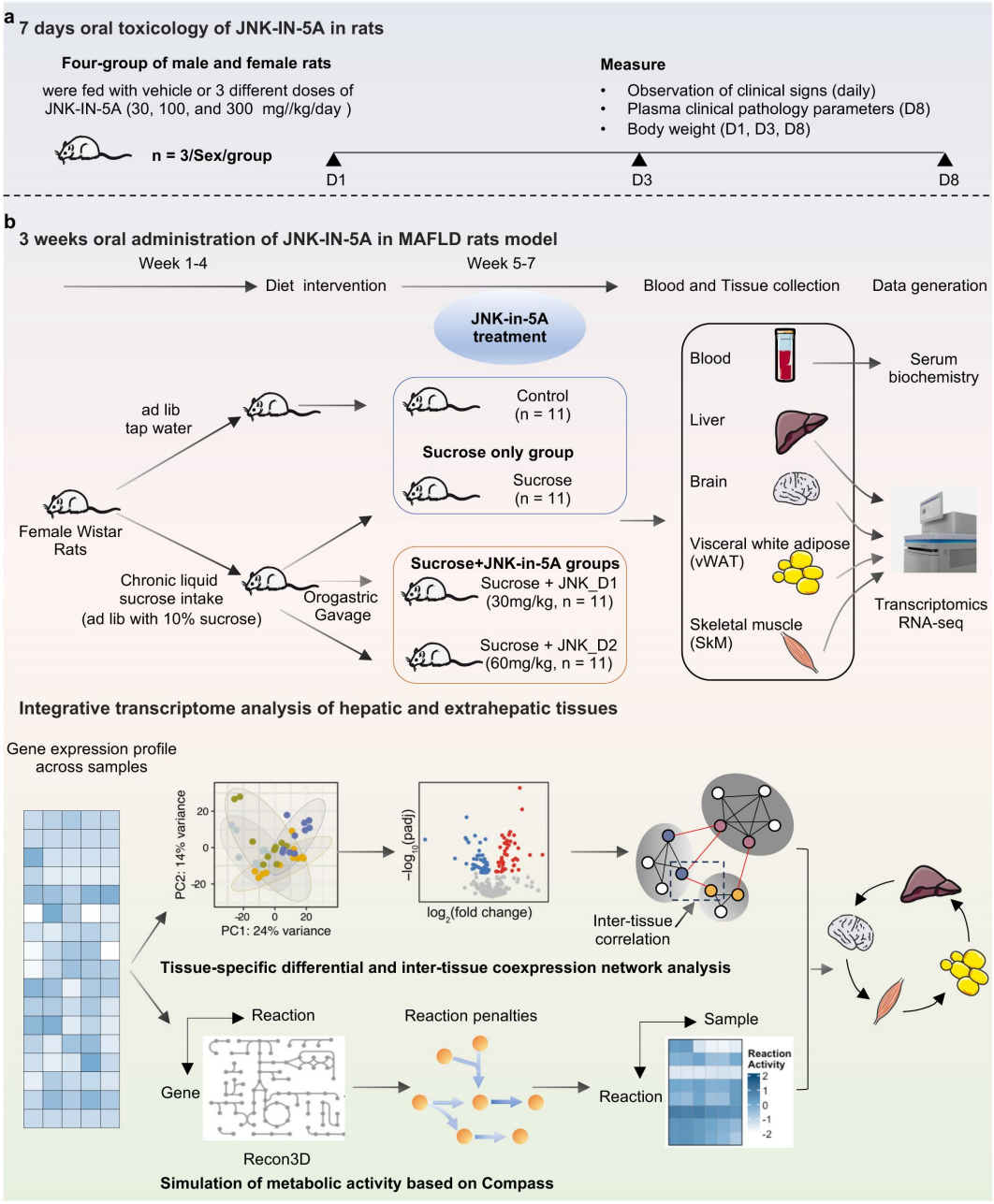

Figure 1.

Schematic representation of experimental setup.

Study groups included the healthy control group received tap water, the sucrose group received 10% sucrose water, the sucrose+JNK_D1 group received 10% sucrose and 30 mg/kg/day JNK-IN-5A, and the sucrose+JNK_D2 group received 10% sucrose and 60 mg/kg/day JNK-IN-5A (N = 44, n = 11 per group).

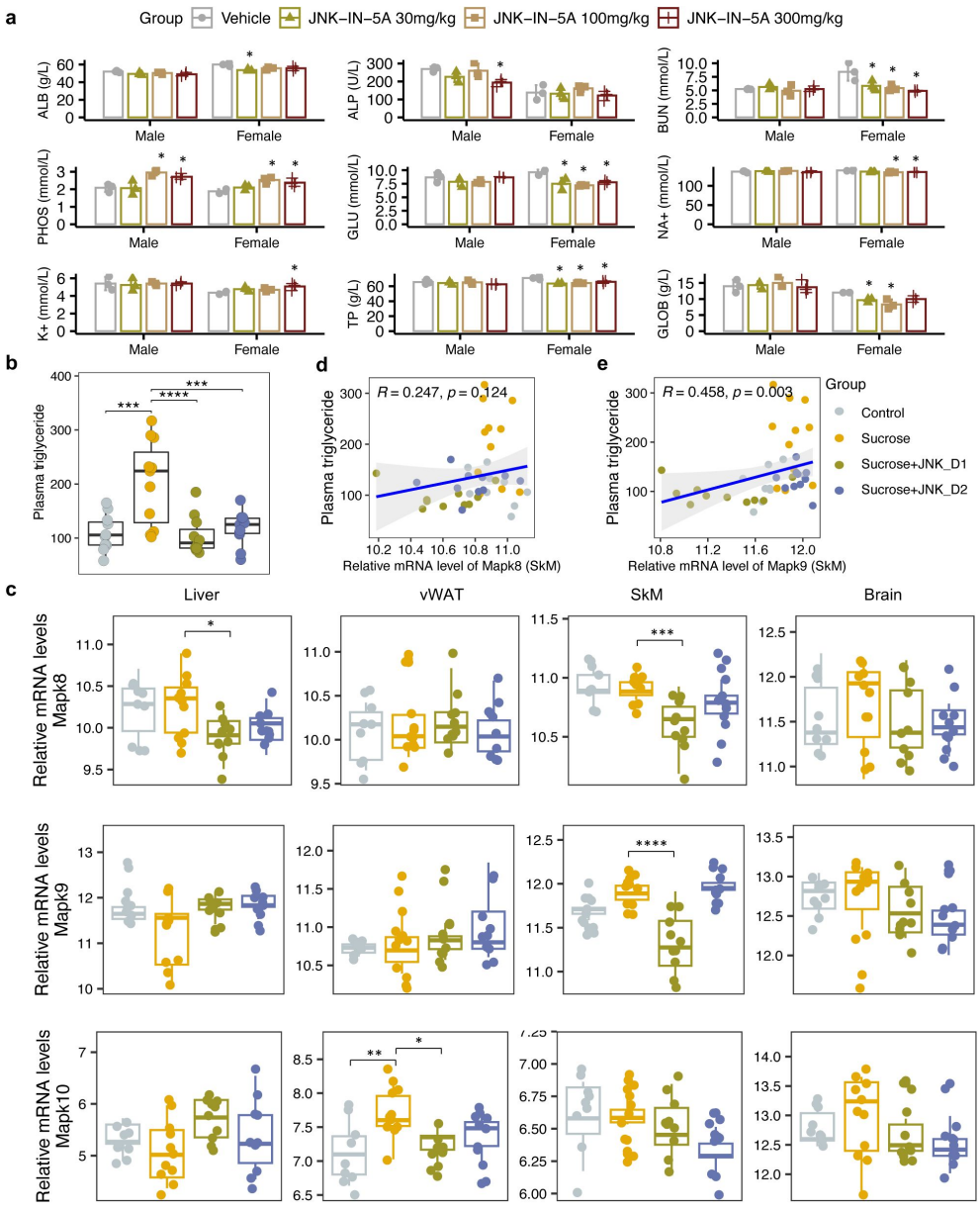

Figure 2.

Sucrose consumption and JNK-IN-5A treatment exhibit distinct effects on the mRNA expression of genes encoding JNK isoforms in the major metabolic tissues.

(a) The acute effect of JNK-IN-5A in rats (n = 3/Sex/Group). Statistically significant changed clinical chemistry parameters were presented as mean ± standard deviation (SD), see also **Data S1**. ALB: albumin; ALP: alkaline phosphatase; BUN: blood urea nitrogen; PHOS: phosphate; GLU: glucose; K^+: potassium; Na^+: sodium; TP: total Protein; GLOB: globulin. Statistical significance was assessed by one-way ANOVA testing followed by Tukey's multiple comparisons post-test or Shapiro–Wilk testing followed by Dunn's post-hoc test, as appropriate, *p*-value < 0.05 is considered as statistical significance. (**b**) Boxplot showing the levels of plasma triglycerides in control, sucrose, sucrose+JNK_D1, and sucrose+JNK_D2 rats. Statistical significance was assessed by one-way ANOVA testing followed by Tukey's multiple comparisons post-test or the Shapiro–Wilk testing followed by Dunn's multiple comparisons post-test, as appropriate, *p*-value < 0.05 is considered as statistical significance. * $p < 0.05$, ** $p < 0.01$, *** $p < 0.001$, **** $p < 0.0001$. (**c**) Boxplot showing the relative mRNA expression of *Mapk8*, *Mapk9*, and *Mapk10* in the studied tissues. The count-based abundance of genes was transformed using the vst function and the adjusted *p*-value (p.adj) is derived from DESeq2 (Love et al., 2014). * p.adj < 0.05, ** p.adj < 0.01, *** p.adj < 0.001, **** p.adj < 0.0001. (**d**) Correlation between the relative mRNA expression of *Mapk8* and (**e**) *Mapk9* in skeletal muscle tissue (SkM) and plasma triglycerides level.

which rats on sucrose watering were further divided into subgroups: sucrose only group and JNK-IN-5A-treated groups at a regular dosage of 30 mg/kg/day (sucrose+JNK_D1 group) or a higher dosage of 60 mg/kg/day (sucrose+JNK_D2 group), for 3-weeks. A total of 44 rats were used in this study (n = 11 rats per group).

We observed that liquid sucrose consumption resulted in significantly increased plasma levels of TG ($p < 0.0001$) and lactate dehydrogenase (LDH, $p < 0.0001$), which is an inflammation marker, compared to the healthy controls (**Fig. 2b**, **Data S2**). On sucrose water, JNK-IN-5A-treated rats exhibited significantly lower levels of TG (JNK_D1, $p < 0.0001$; JNK_D2, $p < 0.001$), aspartate aminotransferase (AST; JNK_D1, $p = 0.09$; JNK_D2, $p = 0.005$), and LDH (JNK_D1, *n.s.*; JNK_D2, $p = 0.015$) but had no significant change on body weight, glucose, high-density lipoprotein (HDL) and low-density lipoprotein (LDL) as compared to their corresponding controls (**Fig. 2b**, **Data S2**). We also performed neurological tests to study the potential effect of JNK-IN-5A on the brain. We found no significant differences among groups in retention latencies, a measure of learning and memory abilities in passive avoidance test (**Data S3**). Additionally, the locomotor activity test was used to analyze behaviors such as locomotion, anxiety, and depression in rat. No significant differences were observed among groups in stereotypical movements, ambulatory activity, rearing, resting percentage, and distance travelled (**Data S4**). Similarly, the elevated plus maze test (Walf and Frye, 2007), an assay for assessing anxiety-like behavior in rodents, showed that rats in all groups had comparable open-arm entries and durations (**Data S5**). Collectively, the behavior tests indicate the JNK-IN-5A-treated rats exhibit no evidence of anxiety and behavior disorders.

To investigate the gene-level inhibition of JNK upon JNK-IN-5A treatment, we further examined the mRNA expression of JNK1 (encoded by the gene *Mapk8*), JNK2 (encoded by the gene *Mapk9*) and JNK3 (encoded by the gene *Mapk10*) in the study. As anticipated, *Mapk8* and *Mapk9* have high expression in all these tissues (liver, vWAT, SkM, and brain) whereas *Mapk10* is highly expressed specifically in the brain tissue (**Fig. 2c**, **Fig. S1a**). Our analysis indicates that the treatment of JNK_D1 effectively alleviated the JNK1 gene expression in the liver ($padj = 0.03$) and exerted more profound inhibitory effects on both JNK1 ($padj = 0.0009$) and JNK2 gene expression ($padj = 2.2e-07$) in SkM (**Fig. 2c**, **Data S6**). Interestingly, we found that plasma TG level is significantly correlated with the JNK2 gene expression in SkM (**Fig. 2d** &**e**). In brain tissue, we found JNK3 gene expression exhibited a trend of dose-dependently inhibition in the JNK-IN-5A-treated groups. Particularly, the downregulation of JNK3 in the sucrose+JNK_D2 group approaches the borderline of significance ($padj = 0.07$), compared to those, which drank sweetened water group only (sucrose group) (**Data S6**).

JNK inhibition rewires metabolic perturbation in the liver and vWAT

To gain in-depth insight into system-level transcriptional response to sucrose consumption and JNK-IN-5A treatment, we next studied the global gene expression profiles in both liver and extrahepatic tissues (vWAT, SkM, and brain). A total of 19,780 protein-coding genes in the rat genome were analyzed (Martin et al., 2023). Principal component analysis (PCA) revealed that liquid sucrose ingestion resulted in the largest transcriptional changes in the liver and vWAT (**Fig. 3a**), which is consistent with previous results (Stephenson et al., 2022). Of note, we observed that JNK-IN-5A treatment, especially JNK_D1, corrected to a large extent of the gene expression profile in the liver and vWAT of treated-rats towards the profile of healthy controls on a principal components space (**Fig. 3a**). In SkM, the transcriptional difference is primally driven by JNK_D1 treatment and showed a clear separation (**Fig. 3a**).

In parallel with the results presented above, differential gene expression analysis revealed that the liver had the largest number of differentially expressed genes (DEGs, DESeq2-Benjamini-Hochberg adjusted $p < 0.01$) associated with liquid sucrose ingestion, comprising a total of 2,771 DEGs (14%), followed closely by vWAT with 2,724 DEGs (13.8%), SkM with 257 DEGs (1.3%), and the

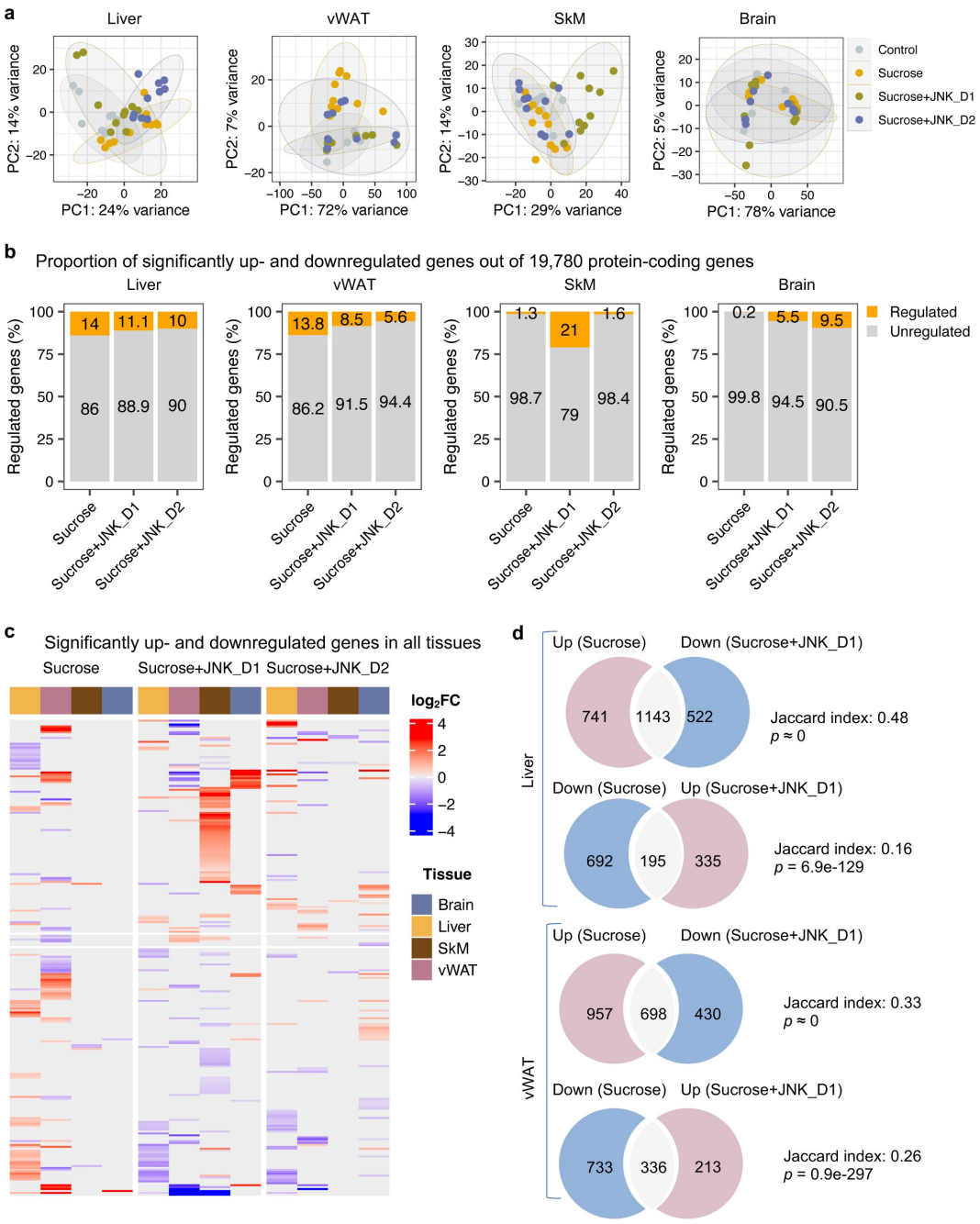

Figure 3.

System-wide transcriptomics profiling revealed tissue-specific metabolic rewiring by sucrose consumption and JNK-IN-5A treatment

(**a**) Principal component analysis (PCA) of liver, vWAT, SkM, and brain transcriptome data showing global gene expression profiles in control (n = 9), sucrose (n = 11), sucrose+JNK_D1 and sucrose+JNK_D2 (n = 10/per group). Each data point represents a sample in the respective coloured group. (**b**) Bar graphs represent the percentage of differential expressed genes (or regulated genes) associated with sucrose (sucrose *vs.* control), sucrose+JNK_D1 (sucrose+JNK_D1 *vs.* sucrose), or sucrose+JNK_D2 (sucrose+JNK_D2 *vs.* sucrose) in all protein-coding genes (N = 19,780) for each tissue. (**c**) Heatmap of all genes differentially upregulated (red) and downregulated (blue) in three pairwise comparisons for sucrose (sucrose *vs.* control), sucrose+JNK_D1 (sucrose+JNK_D1 *vs.* sucrose), and sucrose+JNK_D2 (sucrose+JNK_D2 *vs.* sucrose) (adjusted *p*-value, p.adj < 0.01) for each tissue. Column annotation represents tissues. (**d**) Venn diagram showing the overlap between significantly regulated genes response to sucrose consumption and JNK_D1 treatment, see also **Fig. S1**.

brain with a modest 30 DEGs (0.2%) (**Fig. 3b** &**c**, **Fig. S1b-e**, **Data S6**). Moreover, we observed that JNK_D1 treatment demonstrated a remarkable effect in the reversal of gene expression patterns related to sucrose consumption. Specifically, in the liver, JNK_D1 treatment substantially suppressed the expression of 60.7% (1,143 out of 1,884, hypergeometric $p \asymp 0$) sucrose-induced DEGs and elevated the expression of 22% of sucrose-repressed genes (195 out of 887, hypergeometric p = 6.9e-129) (**Fig. 3d**, **Fig. S1b**). Likewise, we observed a reversal of 42.2% and 31.4% (698 of 1,655 and 336 out of 1,069, respectively) DEGs in vWAT (**Fig. 3d**, **Fig. S1c**). It should be noted that, in both liver and vWAT, the effect of JNK_D2 treatment is relatively smaller than JNK_D1 in terms of the corrections of DEGs (**Fig. S2a** &**b**). Pathway enrichment analysis of JNK_D1 reversed genes identified significantly enriched KEGG pathways related to carbon metabolism, fatty acid metabolism, protein processing in ER, and oxidative phosphorylation (OXPHOS) (Benjamini-Hochberg adjusted $p < 0.01$) (**Fig. S2c** &**d**). Interestingly, some of the genes exhibited opposing regulation in the liver and vWAT in response to the interventions of sucrose only and the combination of sucrose intervention and JNK-IN-5A treatment. This is exemplified in genes related to fatty acid degradation, elongation and biosynthesis (up in the liver and down in vWAT in sucrose only group, while down in the liver and up in vWAT in sucrose plus JNK-IN-5A-treated groups), including *Cpt2*, *Acads*, *Acadvl*, *Acat1*, *Acot5*, *Eci3*, *Hsd17b12*, and *Oxsm* (**Fig. S3**, **Data S6**); genes related to fatty acid (FA) uptake, including fatty acid binding proteins *Fabp1*, *Fabp4* and transporters *Slc27a1* and *Slc27a5* (**Fig. S4**, **Data S6**); and genes related to redox homeostasis, including *Prdx4*, a secreted enzyme that scavenges redox oxidative stress (ROS), *Selenos*, and *Ndufa6* (**Fig. S5**, **Data S6**). Taken together, these results suggest that JNK-IN-5A treatment reshapes sucrose-induced transcriptional changes in both the liver and vWAT, reinforcing their metabolic synergy in FA uptake and metabolism (Stephenson et al., 2022).

JNK inhibition in SkM correlated with the regulation of energy metabolism in the liver and vWAT

It has been reported that JNK acts as a critical mediator of muscle phenotype and adaptive remodelling in animals and humans (Lessard et al., 2018). Here, we found that in contrast to the massive transcriptional regulation observed in the liver and vWAT, liquid sucrose intake has minimal impact on SkM in terms of both genome-wide transcriptional variance (**Fig. 3a**) and the number of DEGs (**Fig. 3a**, **Fig. 4a** &**b**). While in JNK_D1-treated SkM, a substantial quantitative difference in gene expression emerged, encompassing 4,159 (20.9%) DEGs, of which 97% up-regulated (1,552 out of 1,588) and 99% down-regulated (2,557 out of 2,571) genes being exclusively dependent on the JNK_D1 treatment (**Fig. 4a** &**b**). Functional analysis revealed that many of the upregulated genes are involved in immune-related pathways, including hematopoietic cell lineage (HSCs), osteoclast differentiation, chemokine signalling pathway, phagosome, and Fc gamma R-mediated phagocytosis, and down-regulated genes are involved in OXPHOS, thermogenesis, TCA cycle, carbon metabolism, cardiac muscle contraction, and insulin signalling pathway (**Fig. 4c** &**d**, **Fig. 5**). Among the genes regulated by both sucrose-feeding and JNK_D1 treatment in SkM were those involved in the insulin signalling pathway (e.g., *Ppp1r3f*, *Phkg1*, *Phkb*) (**Fig. 5**). As this intra-tissue effect was observed in JNK_D1 not in the JNK_D2-treated group (**Fig. 3b**, **Fig. S5a**), we subsequently investigated the inter-tissue regulation based on the significantly transcriptional changes (as indicated by the $\log_2$-Fold change, $\log_2$FC) in response to JNK_D1 treatment and found that $\log_2$FC of shared DEGs between JNK_D1-treated SkM and liver, vWAT or brain exhibited strong agreements (**Fig. 4e**, **Fig. S5b**). Specifically, 86% and 69% of shared DEGs between SkM and vWAT, and the brain, exhibited consistent changes in response to JNK_D1 treatment (the same $\log_2$FC sign, indicating either upregulated or downregulated in both tissues being compared), with a Spearman correlation of 0.78 and 0.54, respectively. These shared DEGs were found to be involved in several critical metabolic processes, including cholesterol metabolism, bile acid biosynthesis and secretion (such as *Lipc*, *Apob*, *Slc7a1*,

Angptl3, *Slc10a1*), and regulation of energy homeostasis (e.g., *Lep*), suggesting that SkM had a major metabolic adaptation to JNK_D1 treatment and exerts its metabolic effect, at least partially, through coordinated interactions with other tissues.

Inter-tissue network analysis revealed the JNK-IN-5A inhibition-associated molecular mechanism

To better understand the regulation of lipid metabolism and energy homeostasis at a system-wide level in an unbiased manner, we next performed gene co-expression network (GCN) analysis to study intra- and inter-tissue coordination of metabolic pathways as well as biological processes that are associated with sucrose-feeding and/or JNK_D1 inhibition. GCN, a robust systems biology approach (Barabasi and Albert, 1999), allows us to study the functionality of the gene module and its constituent genes. These genes are more likely to be co-expressed if they are either regulated by the same transcription factors or share similar topological properties in protein-protein interaction networks (Califano et al., 2012; Dobrin et al., 2009; Zhang et al., 2016). By investigating the importance and topology of these functional modules, it is possible to understand the biological mechanisms underpinning the disease and/or therapy intervention (Choobdar et al., 2019; Yang et al., 2021; Yang et al., 2014).

We first constructed tissue-specific GCN based on the whole transcriptomics data and selected highly connected genes from the network (the top 10% positively correlated genes that fulfilled FDR < 0.05), followed by module detection using the Leiden clustering algorithm (**Fig. S7a**; **Data S7**). We subsequently evaluated the enrichment of DEGs in the modules to identify those associated with sucrose consumption, JNK_D1 treatment, or both (so-called perturbated module). As expected, GCN analysis revealed distinct gene expression patterns across different tissues (**Fig. 6a**). For instance, in module 1 in the liver (Liver.M1), vWAT.M4, SkM.M4, and Brain.M4, we found a significant enrichment of genes that exhibited elevated expression in response to sucrose consumption while simultaneously being suppressed by JNK_D1. Conversely, Liver.M0 and vWAT.M3 exhibited significant enrichment of genes repressed by sucrose intake but elevated after JNK_D1 treatment. These distinct expression patterns collectively reflect the combined metabolic effect of sucrose-feeding and JNK_D1 interventions. Additionally, GCN analysis identified modules associated with either sucrose-feeding or JNK_D1 intervention at the tissue level, for example, vWAT.M0 (sucrose), vWAT.M1 and Brain.M5 (JNK_D1) (**Fig. 6a**).

To pinpoint gene modules involved in inter-tissue communication, we conducted a correlation analysis among inter-tissue modules using their module eigengene (**see details in Method**) and assessed the enrichment of genes from these modules in MSigDB hallmark gene sets. Our analysis revealed a significant correlation between SkM.M0 and Liver.M0 (R = 0.67, *padj* = 0.006) as well as vWAT.M3 (R = 0.58, *padj* = 0.03) (**Fig. 6b** &**c**). This correlation aligns with the functional annotation of genes within these modules, including those associated with mTORC1 signalling, PI3K/AKT/mTOR signalling, DNA Repair, and unfolded protein response (**Fig. 6d**). Interestingly, we observed that *Mapk9* is among the module members of SkM.M0, indicating a potential metabolic link coordinated by JNK inhibition, connecting SkM with other tissues, including the liver and vWAT (**Fig. 6b**, **Data S7**). SkM.M1 and Liver.M2 (R = -0.66, *padj* = 0.006), SkM.M3 and vWAT.M0 (R = 0.60, *padj* = 0.03), and SkM.M4 and vWAT.M3 (R = -0.66, *padj* = 0.006) were also found to be significantly correlated (R = -0.57, *padj* = 0.03). Note that genes in Liver.M1, vWAT.M3, SkM.M0, SkM.M4, and Brain.M4 are commonly involved in adipogenesis, fatty acid metabolism, OXPHOS, and reactive oxygen species pathway (**Fig. 6d**). These observations suggest the potential crosstalk or regulatory relationship between these tissue modules after JNK_D1 treatment.

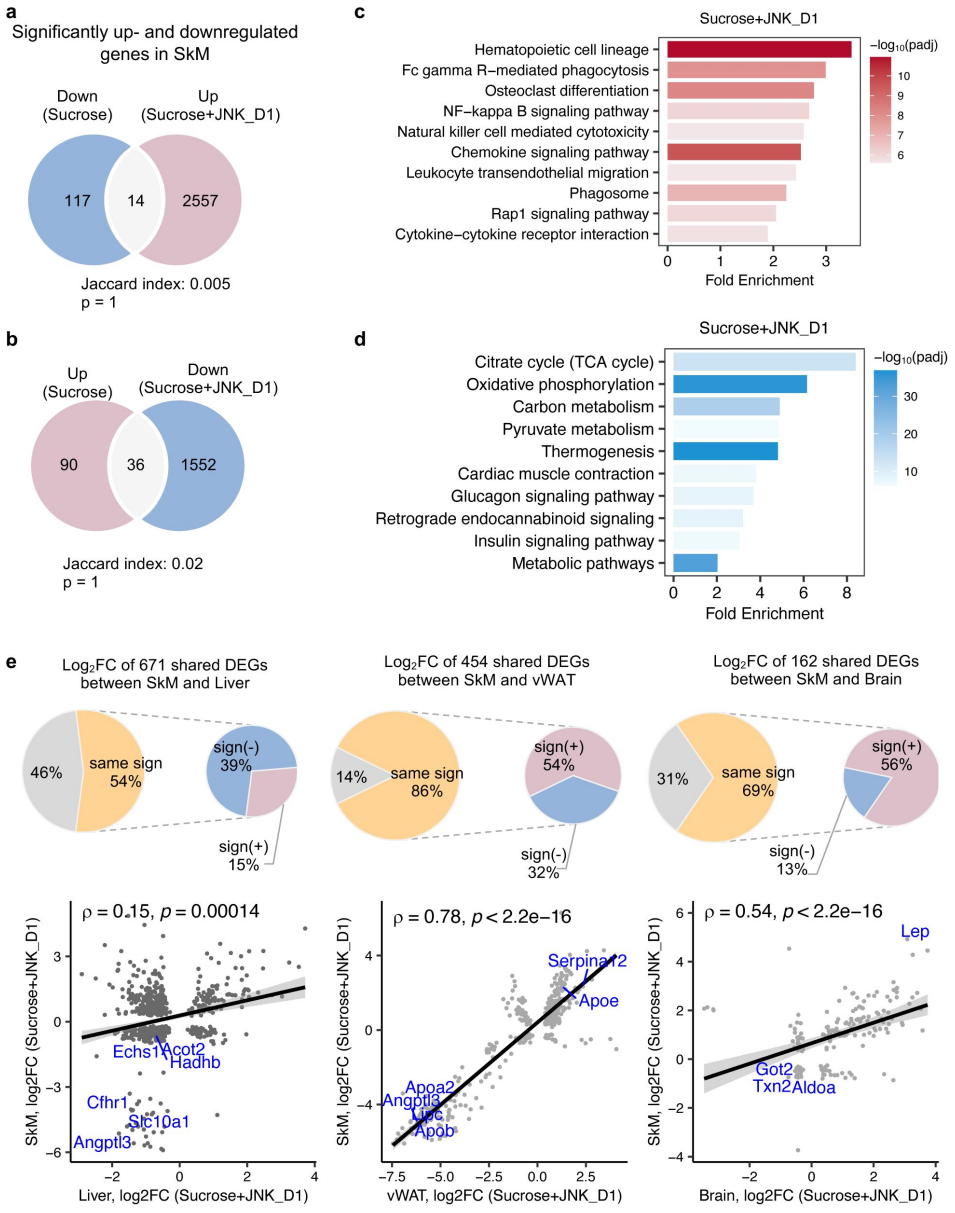

Figure 4.

JNK inhibition in SkM correlated with the regulation of energy metabolism in the liver and adipose tissues.

(**a-b**) Venn diagram showing the overlap between significantly regulated genes response to sucrose consumption and INK_D1 treatment in SkM, see also **Fig. S1** &**Fig. S5**. (**c-d**) Functional annotation of up-(red) and down-regulated (blue) genes in JNK_D1-treated SkM with a Benjamini Hochberg adjusted p-value < 0.05. (**e**) Correlation of $\log_2$(Fold change) for shared DEGs between the SkM and Liver, vWAT, or Brain after JNK_D1 treatment.

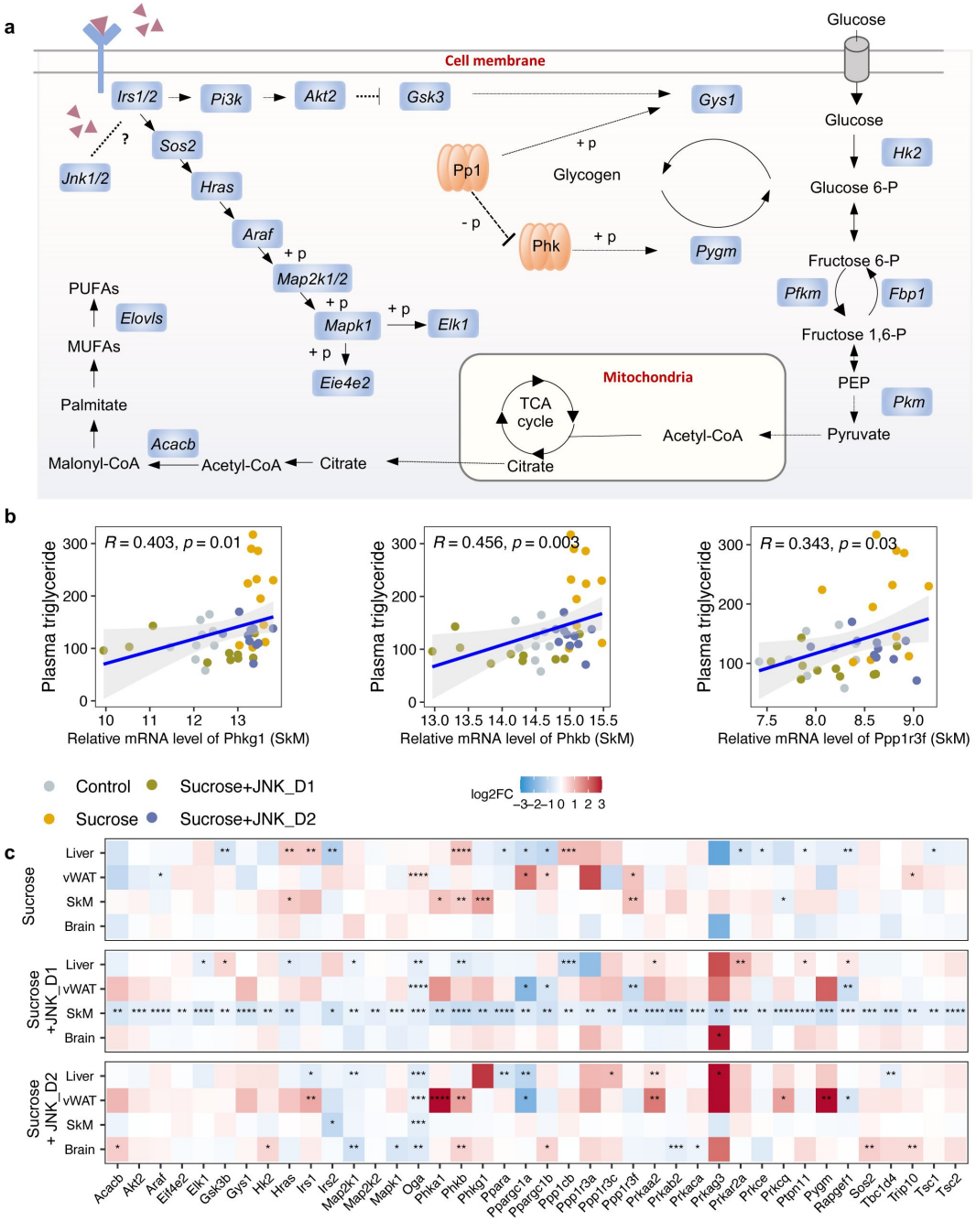

Figure 5.

JNK inhibition regulates insulin signalling-related genes in SkM

(**a**) A representative diagram of metabolic pathways associated with insulin resistance and insulin signalling was found to be largely inhibited by JNK_D1 treatment. (**b**) Correlation between the relative mRNA expression of *Phkg1, Phkb, and Ppp1r3f* (those three genes are also significantly upregulated in sucrose-feeding only group) in SkM and plasma triglycerides level. (**c**) Relative changes of genes involved in insulin resistance and insulin signalling pathways in response to sucrose consumption and JNK-IN-5A treatment in the tissues. The adjusted *p*-value (p.adj) is derived from DESeq2 (Love et al., 2014). * p.adj < 0.05, ** p.adj < 0.01, *** p.adj < 0.001, **** p.adj < 0.0001.

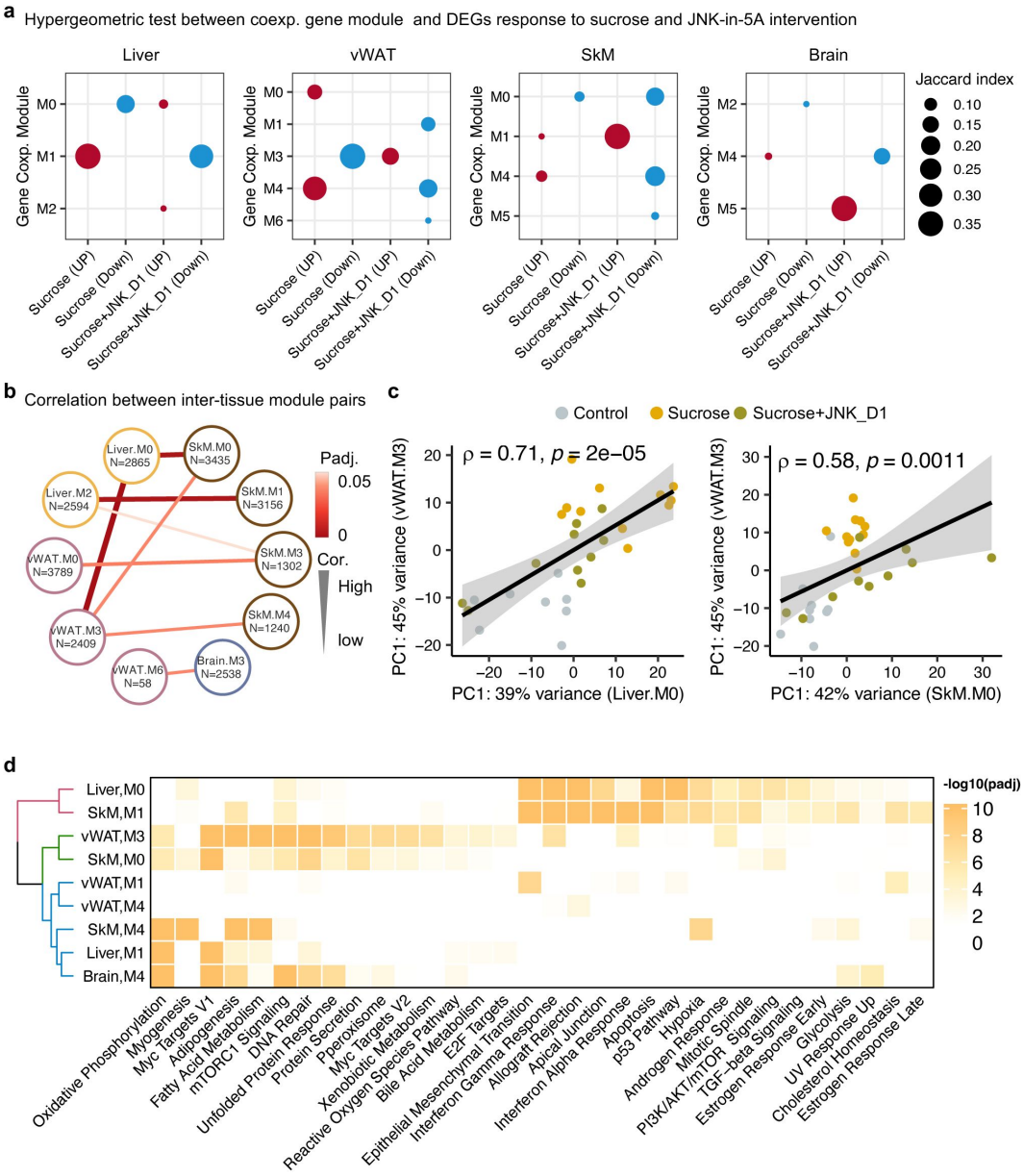

Figure 6.

Inter-tissue network analysis identifies JNK-IN-5A inhibition-associated molecular mechanism.

(**a**) Significantly enriched modules (hypergeometric test, p < 0.05) by the differentially expressed genes related to sucrose, sucrose+JNK_D1 and sccrose+JNK_D1 in each tissue. (**b**) Dot-plot showing the significant correlation among inter-tissue module pairs. The size and colour of the connected line are proportional to the correlation coefficient and statistical significance indicated by the adjusted *p*-value. The module pairs with Benjamini Hochberg adjusted p-value (p.adj) < 0.05 are presented. (**c**) Spearman coefficient correlation of the first component from PCA analyses on gene expression of module pairs. (**d**) Significantly enriched MSigDB hallmark gene sets by each module.

Metabolic modelling identified the metabolic reprogramming linked to JNK-IN-5A inhibition

To predict how tissue-level metabolic activity responds to sucrose feeding and JNK-IN-5A treatment, we performed an integrative analysis of transcriptomics data by generating tissue-specific GEMs and applying Compass (Wagner et al., 2021). Compass is a flux balance analysis-based (Orth et al., 2010) algorithms to model the metabolic state of a system (e.g., single cell or tissue), taking into account the observed expression levels of enzyme-coding genes in each sample from RNA-seq data. In this study, we employed Recon3D, a generic GEMs of human metabolism, comprising 10,600 metabolic reactions associated with 5,835 metabolites and 2,248 metabolic genes (Brunk et al., 2018). Consistent with our previous analysis, we observed a shift in metabolic activity in the liver and vWAT after JNK_D1 treatment (**Fig. 7**, **Data S8**). Specifically, Compass predicted that 2,840 and 4,170 metabolic reactions showed significantly altered activity (Wilcoxon test, adjusted p-value < 0.05) following the sucrose consumption in the liver and vWAT, respectively. 89.2% and 88.3% of which were correspondingly reversed after JNK_D1 treatment (**Data S8**). The common altered reactions are partitions into the subsystems named citric acid cycle, fatty acid oxidation, fatty acid synthesis, and tryptophan metabolism in Recon3D (**Fig. 7c**). Some of the predicted metabolic changes align with previous findings in rodents subjected to sucrose overconsumption. For example, Öztürk et al. reported altered tryptophan metabolism in rats consuming 10% sucrose in drinking water, including decreased serum levels of kynurenic acid and kynurenine (Eryavuz Onmaz and Ozturk, 2022). Similarly, increased triglyceride-bound oleate, palmitate, and stearate were observed in the livers of rats fed a 10% sucrose solution (Stephenson et al., 2022), indicating JNK-IN-5A treatment may regulate lipid metabolism by modulating these metabolic activities. Moreover, we found 8 metabolic reactions significantly altered in sucrose+JNK_D2-treated rats, including 2 reactions involved in glycolysis/gluconeogenesis, 2 in nucleotide interconversion, 1 in pentose phosphate pathway, 1 in fructose and mannose metabolism, 1 in propanoate metabolism (Cohen's d < 0, padj < 0.05), and 1 in drug metabolism (Cohen's d > 0, padj < 0.05) (**Data S8**). Hence our systems biology analysis revealed the molecular mechanisms altered due the JNK-IN-5A treatment.

Discussion

The etiology of MAFLD is multifactorial and remains incompletely understood, impeding the progress in developing effective therapies for MAFLD. Our investigation into the metabolic changes from the major metabolically active tissues enabled us to systematically assess the potential therapeutic effects of JNK-IN-5A under high sucrose consumption. Here, we demonstrated that JNK-IN-5A attenuated the accumulation of circulating TG and inflammation exaggerated by liquid sucrose consumption. Importantly, the rats treated with JNK-IN-5A did not exhibit indications of anxiety or behavioural disorders. These results have important implications for the development of JNK3 inhibitors, taking into account the high expression of JNK3 in the brain (Chang and Karin, 2001). Additionally, our data indicated that JNK-IN-5A, a selective inhibitor of JNK2 and JNK3 (Angell et al., 2007; Cerbone et al., 2012), also exerted an inhibitory effect on the gene expression of JNK1 in *in vivo*, especially in skeletal muscle (**Fig. 2**).

By studying the hepatic and extrahepatic tissues using genome-wide transcriptome data and integrative analyses with GEMs, we found that the intervention with sucrose-sweetened water triggered extensive transcriptional changes in the liver and adipose tissues, including those involved in fatty acid and oxidative metabolism. The metabolic axis between the liver and adipose tissues is a critical regulatory network that governs energy balance and metabolic homeostasis in the body (Azzu et al., 2020). It has been reported that upon chronic overnutrition, adipose lipogenesis is significantly downregulated, which leads to ectopic lipid accumulation and insulin resistance (Jeon et al., 2023). In line with this, we found that in the sucrose-sweetened water

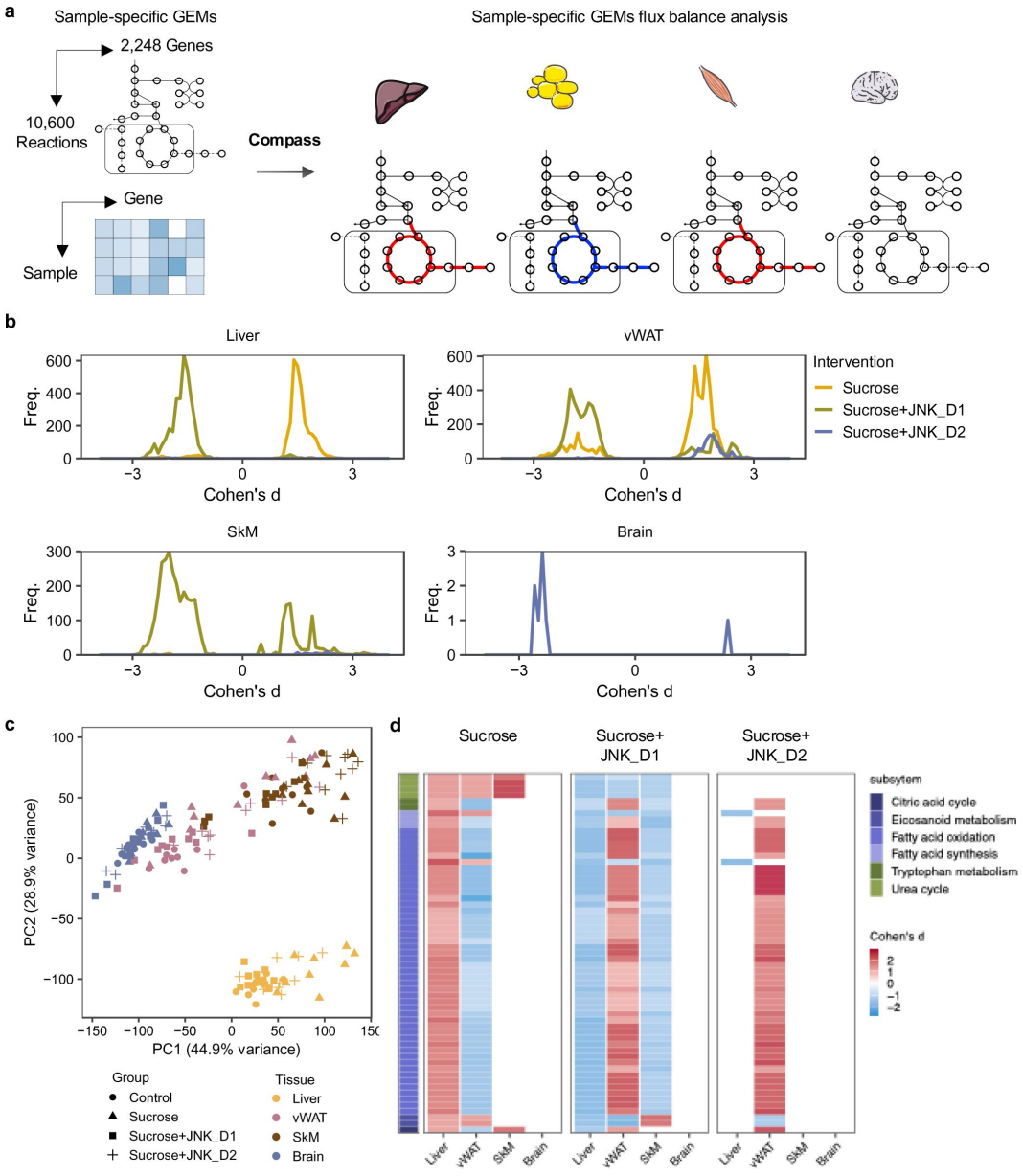

Figure 7.

Metabolic modelling highlights metabolic reprogramming linked to JNK-IN-5A inhibition

(**a**) Simulation of metabolic activity based on Compass (Wagner et al., 2021) and Recon3D (Brunk et al., 2018). (**b**) Distribution of Cohen's d statistic for differential metabolic reactions in response to sucrose, sucrose+JNK_D1 and sucrose+JNK_D2 in each tissue, see also **Data S8**. (**c**) Principal component analysis of the Compass score of metabolic reaction potential activity scores showing the metabolic heterogeneity in response to sucrose ingestion and JNK-IN-5A treatment at the tissue levels, for principal components 1 and 2. (**d**) Heatmap showing the tissue-level differential activity of metabolic reactions in response to sucrose intake and JNK-IN-5A treatment. Reactions are partitioned by Recon3 pathways (Brunk et al., 2018) and coloured by the sign of their Cohen's d statistic derived from different contrasts: sucrose *vs* control, sucrose+JNK_D1 *vs* sucrose, or sucrose+JNK_D2 vs sucrose, respectively. Abbreviations: vWAT, visceral white adipose tissue; SkM, skeletal muscle.

group, the mRNA expression of many genes related to fatty acid metabolism and uptake is downregulated in adipose tissue. Interestingly, those genes showed the opposite regulation between liver and adipose tissue, indicating their complementary role in these metabolic processes in response to the diet intervention. These findings also pinpoint the critical role of extrahepatic metabolism in the development of MAFLD.

JNK plays essential roles in a range of signalling pathways that have implications for metabolic processes such as insulin sensitivity, thermogenesis, adipogenesis, and lipid metabolism (Nikolic et al., 2020; Solinas and Becattini, 2017). Our data demonstrated that JNK-IN-5A, especially when administered at a regular dosage (JNK_D1, 30mg/kg/day), effectively opposite a substantial portion of the transcriptional changes induced by sucrose consumption, particularly those related to carbon, fatty acid metabolism, OXPHOS, and thermogenesis in the liver and adipose tissues. This suggests that JNK-IN-5A might hold promise as a potential strategy for restoring metabolic perturbation in tissues challenged by sucrose-induced stress. However, our study also revealed that JNK_D1-treated skeletal muscle exhibited profound transcriptional changes related to HSCs, osteoclast differentiation, and immune-related pathways. Importantly, we found that these changes were not confined to skeletal muscle but exhibited correlations with transcriptional changes in the liver, adipose tissue, and even brain tissue. The suggest the coordinated roles of JNK inhibition in mitigating sucrose-induced MAFLD across these tissues, while the exact molecular mechanisms by which JNK-IN-5A exert its muscle-specific effect warrant further investigations. Previously, Xiao *et al.* (Xiao et al., 2019) demonstrated that the JNK pathway regulates HSCs expansion and self-renewal in JNK-IN-8-treated $CD34^{+}CD45RA$-CB cells. Lessard *et al.* (Lessard et al., 2018) demonstrated that mice with muscle-specific JNK1/2 knockout, have a muscle phenotype that mimics that of endurance-trained athletes. Together with our data, these results suggest a multifaceted role of JNK signalling in the regulation of HSCs and metabolism in skeletal muscle.

Although overactivated JNK activity presents an attractive opportunity to combat MAFLD, inhibition of JNK presents substantial challenges and potential risks due to its broad and multifaceted roles in many cellular processes. One key challenge is the dual role of JNK signaling (Lamb et al., 2003). For instance, long-term JNK inhibition may disrupt liver regeneration, as JNK plays a critical role in liver repair by regulating hepatocyte proliferation and survival following injury or stress (Papa and Bubici, 2018). In HCC, it has been reported that JNK acts as both a tumor promoter, driving inflammation, fibrosis, and metabolic dysregulation, and a tumor suppressor, facilitating apoptosis and cell cycle arrest in damaged hepatocytes. Its inhibition, therefore, carries the risk of inadvertently promoting tumor progression under certain conditions (Seki et al., 2012). Furthermore, the differential roles of JNK isoforms (JNK1, JNK2, JNK3) and a lack of specificity of JNK inhibitors present another layer of complexity. Given these challenges, while our study demonstrated the potential of JNK-IN-5A in mitigating early metabolic dysfunction in the liver and adipose tissues, JNK targeting strategies should be carefully tailored to the disease stage under investigation. For curative approaches targeting advanced MAFLD, such as MASH, future studies are warranted to address considerations related to dosing, tissue specificity, and the long-term effects.

In summary, our study provides a comprehensive understanding of the therapeutic potential of JNK-IN-5A treatment in a rat model of sucrose-induced MAFLD. Through an analysis of genome-wide transcriptome data in the major metabolic tissues, we shed light on the JNK-IN-5A-mediated metabolic effects in both hepatic and extrahepatic tissues. This implies a potential therapeutic strategy for the treatment of diet-induced MAFLD and other metabolic complications, potentially by regulating cellular energy homeostasis and mitochondrial metabolism. Nevertheless, several limitations warrant consideration. First, while we observed transcriptional adaptations in skeletal muscle tissue following treatment, the exact molecular mechanisms underlying these changes and their roles in skeletal muscle function and systemic metabolic homeostasis remain unclear. Further investigation is warranted to elucidate the muscle-specific effects of JNK inhibition.

Second, our study did not investigate the dose-dependent or potential off-target effects of JNK-IN-5A, particularly its activity on other members of the kinase family and associated signaling pathways. Lastly, the long-term effects of JNK-IN-5A administration remain unexplored. Understanding its prolonged impact across different stages of MAFLD, including advanced MASH, is crucial for assessing the full therapeutic potential of JNK inhibition in the treatment of MAFLD.

Materials and Methods

Experimental models and subject details

1. Oral Toxicity Study in Rats

Twelve male and twelve female rats of the Wistar strain (Envigo, Venray, Netherlands) were used to assess the 7-day oral (gavage) toxicology, in terms of clinical signs, body weight and clinical pathological parameters, of JNK-IN-5A in rats. Animals were group-housed under standard conditions and had free access to water and 2916C Teklad global 16 % protein rodent irradiated diet (Envigo, Venray, Netherlands). Dose levels of 0 (vehicle control), 30, 100, or 300 mg/kg of JNK-IN-5A were administered once daily via oral gavage for 7 days. The vehicle was 2 w/w% HPMC (Colorcon), 2 w/w% PS80 (Merck) in 10 mM PBS, pH 7 and dose volume was 5 mL/kg for JNK-IN-5A. Body weights were recorded the week before and within 24 hours before the start of dosing and on Day 3 and on necropsy Day 8. All animals were bled at 2 hours after dosing on Day 1 and Day 7. Blood samples were placed on ice after sample collection and centrifuged at approx. 3000xG, 5 min., 4°C. 7.5 µL plasma was transferred into a separate low-binding protein tube and the remaining plasma was transferred into a second low-binding tube. The tubes were frozen upright at approximately - 20°C. Blood and plasma were analysed using an Exigo analyser and Vetscan equipment. The VetScan analyser was calibrated with calibration samples with known plasma levels of each parameter before the start of analysis, occasionally during the analysis period of study samples and after completed analyses. All the animal procedures (including housing, health monitoring, dosing, etc.) and ethical revisions were performed according to the 2010/63/EU Directive on the protection of animals used for biomedical research.

2. JNK-IN-5A Treatment Study in Rats

All experiments were performed in accordance with institutional ethical guidelines, and the present in vivo study was approved by the Ethics Committee for Animal Research of Atatürk University (with the reference number 2023/04 on 30.03.2023). Rats were obtained from the Atatürk University Experimental Research Center. All groups were housed on a 12-hour light and dark cycle. The temperature and humidity values of the environment were kept at optimal values. To prevent neophobia, rats were divided into groups one week before sucrose treatment by following the double-blind method to adapt to the laboratory environment and each other.

A total of 4 groups consisting of 11 subjects each were formed, including the healthy Control group consisting of rats received ad libitum tap water, the Sucrose group consisting of rats received ad libitum 10% Sucrose (BioShop, Canada, Lot No: 2E77269) (equivalent to the concentration of fructose in typical soda (Jang et al., 2020)), and groups treated by JNK-IN-5A at two concentration: sucrose+JNK_D1 group with rats received ad libitum 10% sucrose and 30 mg/kg/day JNK-IN-5A gavage and sucrose+JNK_D2 group with rats received ad libitum 10% sucrose and 60 mg/kg/day JNK-IN-5A gavage. The rats had ad libitum access to tap water (Control) or 10% sucrose water (sucrose, sucrose+JNK_D1, and sucrose+JNK_D2) and a standard chow diet throughout the experimental period. The amount of water consumed by all groups was recorded daily, and drinking water was renewed every day. After feeding with sucrose for 4 weeks, drug treatment was given at the following 3 weeks. Behavioural tests were taken before the experiment started and after 3 weeks of drug treatment. Locomotor activity tests, elevated plus maze tests and passive

avoidance tests were used as behavioural tests. Behavioural tests were repeated at the end of the 21-day treatment regimen. While the last behavioural tests were being taken, drug treatment continued so that the drug level in the blood would not change. After the experimental animals were sacrificed with a high dose (200 mg/kg thiopental sodium) anaesthetic, the relevant tissues were taken for further analysis.

2.1 Monitoring behaviour

All tests were performed twice in total, initially and after the 21-day treatment regimen. According to the results obtained from the initial measurements, rats with outliers for the experiment were determined. After the treatment measurement, it was determined whether there was any change in the behaviour of the rats. The **Locomotor Activity Test** is a system used to test differences in motor activity and anxiety-related behaviours of rats. In the system scanned with infrared rays, each of the ambulatory, stereotypical, rearings, resting percentage and travelled distance movements of the rats are digitized and converted to computer output. These outputs are evaluated and provide information that needs to be interpreted about the animal's adaptation to the new environment and the continuation of the sense of curiosity or anxiety. Stereotypical movement shows rats grooming and recognizing their environment. Ambulatory movement is all the movements that rats make on the ground without standing up. Distance shows the distance travelled by the rats in the cage. The rearing movement indicates the time the rats stand up in the cage. The resting percentage is an indicator of anxiety. Ambulatory movements are recorded with horizontal sensors that surround the cage 360 degrees at the base, and stereotypic and rearing movements are recorded with vertical sensors located 10 cm above the floor. The entire cage continues to be measured continuously with 250 ms infrared. Unlike the open field test, activity measurement is performed in this study and the computer automatically records all the recordings instead of an independent observer (Lu et al., 2019). The experiment is performed in a dark environment. Rats are placed in cages for 10-minute periods and the system automatically records with infrared rays. After each rat, the cage is cleaned with alcohol to remove odor and urine (Ferah Okkay et al., 2022). **The Elevated Plus Maze Test** is used to measure anxiety-like behaviour in rodents. The elevated plus maze apparatus is a system consisting of two open arms (without walls; 50 cm × 10 cm) and two closed arms (with black walls, 50 cm × 10 cm). The open and closed arms are connected by a central platform. The labyrinth is 55 cm above the ground. At the start of each test, rats are placed in the central zone and allowed to explore the platform for 5 minutes. The rats are recorded with a camera located at the top of the maze and the test is done in a quiet, dim room. The number of times the rats entered the open and closed arms, and the time spent in these arms were recorded. The device was cleaned with an alcohol solution between tests (Chellian et al., 2020; Walf and Frye, 2007). Results are given as arm entries and time spent (durations) in these areas. The more entries into open arms and the more duration spent there, the less anxiety the rat has. The **Passive Avoidance Test** is a system consisting of 2 rooms (light/dark), the base of which is covered with rods that can apply electroshock, in which memory, behaviour and learning abilities are investigated. This system is used to test the learning ability of the animal by fear-driven conditional avoidance. In this test, the animal is expected to learn to avoid entering the electroshock chamber (dark room). Rats are nocturnal animals. By nature, they sleep during the day and are active at night. Although rats are not afraid of light, they generally live in dark compartments because they are uncomfortable with the bright environment. In the passive avoidance system, lighting the bright compartment with LED lights and high lumen light creates an uncomfortable environment for the animals, and they want to move to the closed compartment. Here, the low intensity electroshock they are exposed to causes a deterrent stimulus and allows the rats to understand and learn how the system works. The experimental procedure is built on these understanding and learning abilities (Gimenez De Bejar et al., 2017; Hosseini et al., 2013; Wu et al., 2020). The experiment is carried out on two consecutive days. Learning is measured on the first day and recall on the second day. The time that each rat took to enter the dark compartment was considered as initial latency. The next day (retention phase), the rats were reintroduced into the bright chamber and the step-through latency was noted down as memory retention. Shorter latencies indicated poorer cognition. At this stage, rats are expected to

remember the shock in the dark compartment. For this reason, it was accepted that the memory of the rats that stayed longer in the bright compartment was stronger. In retention measurements, it is understood that the longer the rats stay in the bright compartment, the stronger the memory and learning.

2.2 RNA extraction and library preparation for transcriptome sequencing

Total RNA is extracted from the snap-frozen rat tissues with Zymo Research Quick RNA Miniprep kit (California USA) by following the protocol provided on the manufacturer's website with slight modifications made to improve the quality and quantity of RNA from each tissue. Before the cell lysis, the tissues are subjected to short (1 min or longer for muscle tissues) homogenization with the beads in PowerLyzer 24 by keeping samples on ice to prevent overheating. The homogenized tissues are further enzymatically in a digestion buffer for at least 30 minutes or more for muscle tissue at room temperature with continuous inversion and agitation of the tubes. After the lysis of the cells, the RNA is cleaned and collected with columns. The quality and quantity of the isolated samples were examined spectrophotometrically with NanoDrop (Thermofisher, USA). After the evaluation of the sample A260, A260/A280, and A260/A230 values, the RNA integrity number (RIN) value of total RNA samples was measured with TapeStation (Agilent Tech, USA). The amount of total RNA was measured more precisely fluorometrically with the RNA Broad Range kit (Thermofisher, USA) by using Qubit (Invitrogen, USA). RNA sequencing library was prepared with Illumina Stranded Total RNA Prep and Ligation with Ribo-Zero Plus kit was used by following the standard protocol provided by the manufacturer. The libraries were then pair-end (2×100bp) sequenced on the NovaSeq6000 system yielding, on average, 25 million fragment reads per sample. Raw sequencing data (.bcl) was converted to FASTQ with the Dragen Bio-IT platform (v3.9.5). The quality of RNA-seq data was assessed by FastQC (v0.11.9).

2.3 RNA-seq data processing, differential expression, and functional enrichment analysis

Tissue bulk RNA-seq data were aligned and quantified using a standard protocol of Kallisto (v0.46.2) (Bray et al., 2016) against the *Rattus norvegicus* genome (mRatBN7.2) downloaded from Ensembl (Martin et al., 2023) official website (*https://www.ensembl.org/index.html*). The output of Kallisto, both estimated counts and TPM (transcript per kilobase million)-based transcript-level expressions were then transformed into gene-level expressions using the Bioconductor package tximport (v1.22.0) with the tx2gene option set to connect transcripts to genes (Soneson et al., 2015). Protein-coding genes were considered for the above step and downstream analyses. Differential analysis was performed using the DESeq2 Bioconductor package (v1.34.0) (Love et al., 2014), following a standard protocol for all three pairwise intervention comparisons for determining the effect of sucrose consumption only (sucrose *vs* control), the effect of 30 mg/kg/day JNK-IN-5A treatment (sucrose+JNK_D1 *vs* sucrose), and effect of 60 mg/kg/day JNK-IN-5A treatment (sucrose+JNK_D2 *vs* sucrose) in all four studied tissues. Significantly expressed genes (DEGs) were identified with a significance threshold of an adjusted p-value < 0.01. To examine differences in global gene expression, we conducted principal component analysis (PCA) based on variance-stabilizing transformation (VST)-normalized count data in DESeq2. PC1 and PC2 were plotted for visualization.

Gene Co-expression Network Analysis

For the generation of the tissue-specific co-expression networks, we first filtered out lowly-expressed genes based on their TPM-based expression level (TPM <1) and constructed co-expression networks by generating gene pairs Spearman correlation ranks within the tissue, which was performed using the "spearmanr" function from *SciPy* (Virtanen et al., 2020) in Python 3.8. Next, considering the network with negative correlation has relatively low correlation scores, we retained the top 10% positively correlated genes that fulfilled FDR < 0.05 on the network (Arif et al., 2021; Yang et al., 2021) and performed module detection analysis using Leiden algorithm (Traag et al., 2019), implemented in the *leidenalg* (v0.7.0) package with

"ModularityVertexPartition" to find the optimal partition. Modules with less than 30 genes were discarded to be able to get significant functional analysis results in the downstream analysis. To identify gene modules involved in tissue crosstalk, we correlated the module eigengenes of inter-tissue modules and assessed the significance of these correlations after Benjamini & Hochberg (BH) correction, with BH-adjusted $p < 0.05$ was considered as significance. The module eigengene is defined as the first principal component of the expression matrix of a given module.

Gene Set Functional Enrichment Analysis

we used Bioconductor package enrichR (v3.2) to annotate gene sets (e.g., differentially expressed genes or co-expression genes) against the curated genes sets obtained from the KEGG pathway database (Kanehisa, 2002), or against hallmark gene sets from MSigDB (Liberzon et al., 2015) using R package msigdbr (v.7.5.1). Benjamini-Hochberg (BH)–adjusted P values (p.adj) < 0.05 are considered as statistically significant and are provided in the relevant figures/datasets.

2.4 Compass-based Metabolic Activity Analysis

We inferred tissue-level metabolic state from RNA-seq profiles using Compass (Wagner et al., 2021). Compass is a flux balance analysis-based algorithm (Orth et al., 2010) that enables modeling the metabolic state of a system (e.g., single-cell or organ) from RNA-seq data based on a reconstructed genome-scale metabolic model of human metabolism (also known as Recon3D) (Brunk et al., 2018). We downloaded Recon3D from BiGG Models (*http://bigg.ucsd.edu/models/Recon3D/*) and created model metadata files required for the input of downstream analysis, including gene, reaction, and metabolite metadata, using in-house scripts. We used human orthologs of rat gene expression data (TPM-based) for computation of the Compass scores matrix using default parameters, and the human species as detailed in (Wagner et al., 2021). Downstream analysis was done using the compassR R package (v.1.0.0) following the protocol (*https://github.com/YosefLab/compassR*).

Statistical Analyses

Data were shown as mean ± standard deviation (SD), unless stated otherwise. The assumption of normality for continuous variables from behavior test, biometric measurements, and plasm biochemistry was determined using the Shapiro–Wilk test. Differences among multiple groups were tested by ANOVA or, for data that were not normally distributed, the non-parametric Kruskal-Wallis test. Pairwise comparisons were performed using Tukey's post hoc test following the ANOVA or Dunn's multiple comparisons post hoc test following the Kruskal-Wallis test, as appropriate. The Jaccard index was used to evaluate the similarity and diversity of two gene sets, and a hypergeometric test was used to test the significance of their overlap. All results were considered statistically significant at $p < 0.05$, unless stated otherwise.

Supplementary Figure Legends

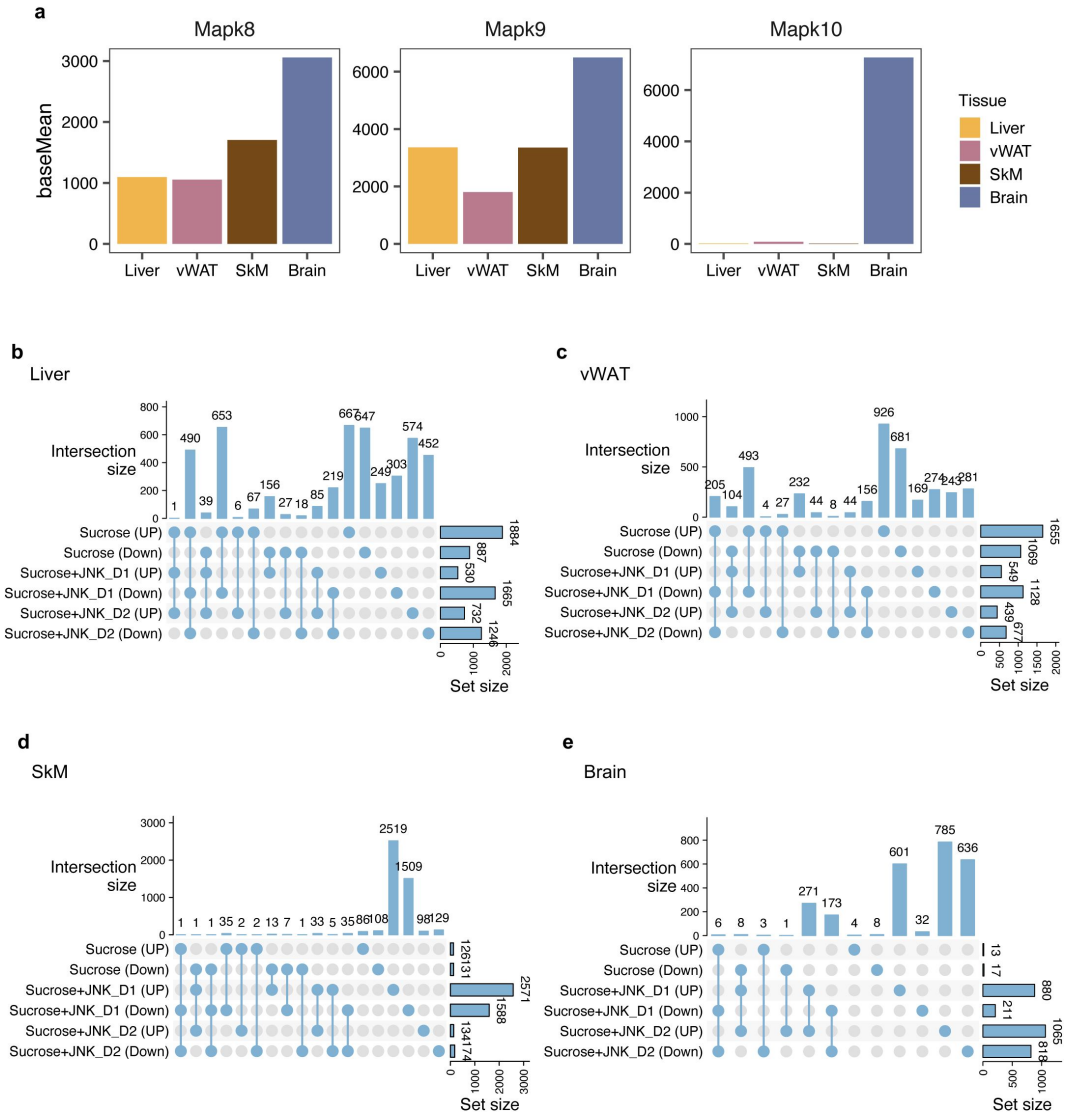

Figure S1.

(**a**) Gene expression pattern of JNK isoforms (**b-e**) UpSet plot showing the number of shared differentially expressed genes (DEGs) (adjusted-p < 0.01) associated with sucrose consumption and JNK-IN-5A treatment in the liver, visceral white adipose tissue (vWAT), skeletal muscle tissue (SkM) and brain tissues in the experimental rats. The histogram bar graph (right) shows the total number of DEGs in each comparison corresponding. The histogram bar graph (top) shows the number of DEGs shared among pairwise comparisons. Connected lines indicate what comparisons are sharing DEGs.

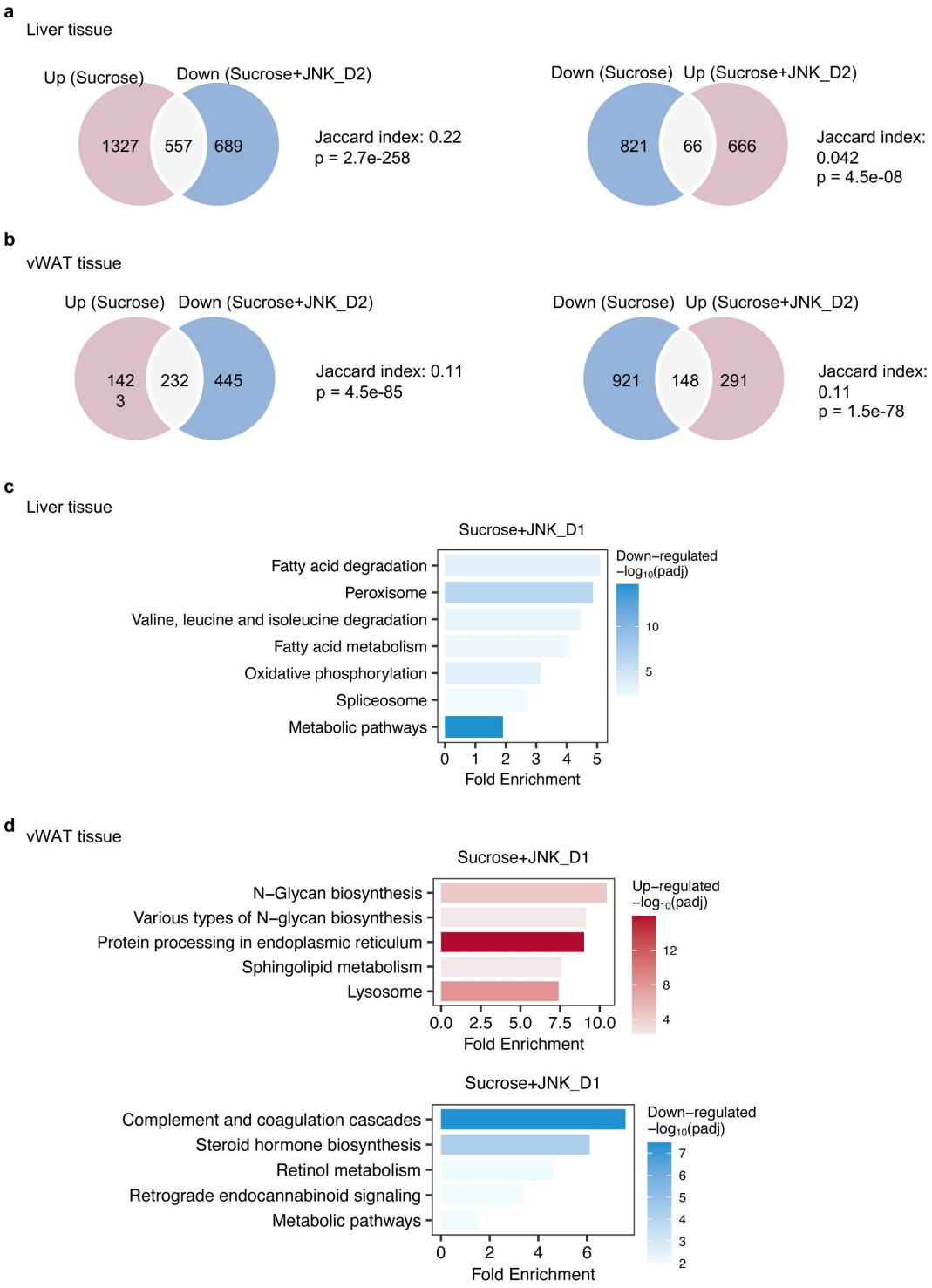

Figure S2.

(**a**) Venn diagram showing the overlap between significantly regulated genes response to sucrose consumption and JNK_D2 treatment in liver and (**b**) in vWAT, related to **Fig. 3**. (**c**) Top-10 enriched KEGG pathways enriched by reversed genes after JNK_D1 treatment in liver and (**d**) in vWAT.

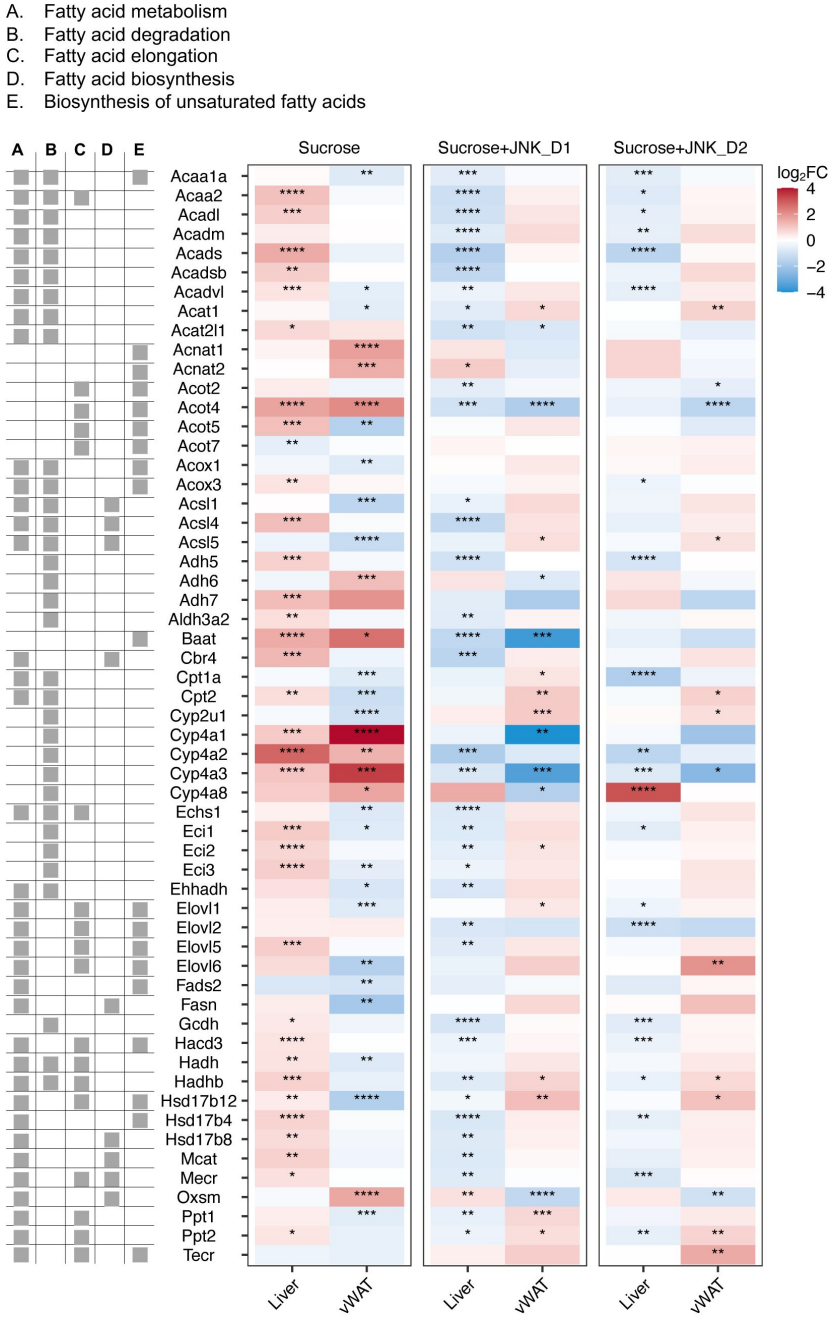

Figure S3.

Relative changes of genes involved in fatty acid degradation, elongation, biosynthesis, and metabolism in response to sucrose consumption and JNK-IN-5A treatment in the tissues, related to **Fig. 2**.

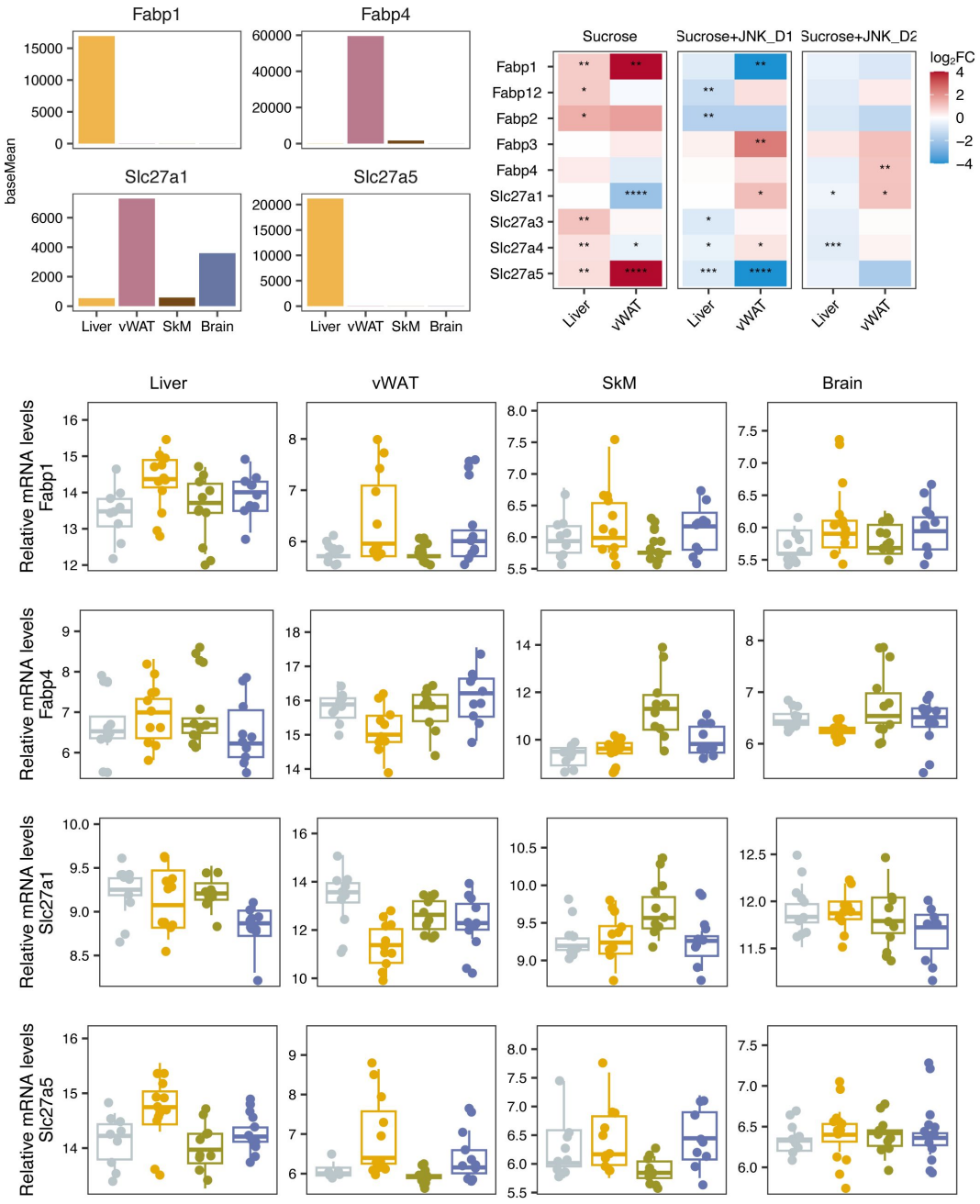

Figure S4.

Relative changes of genes involved in fatty acid uptake in response to sucrose consumption and JNK-in-5A treatment in the tissues, related to **Fig. 2**.

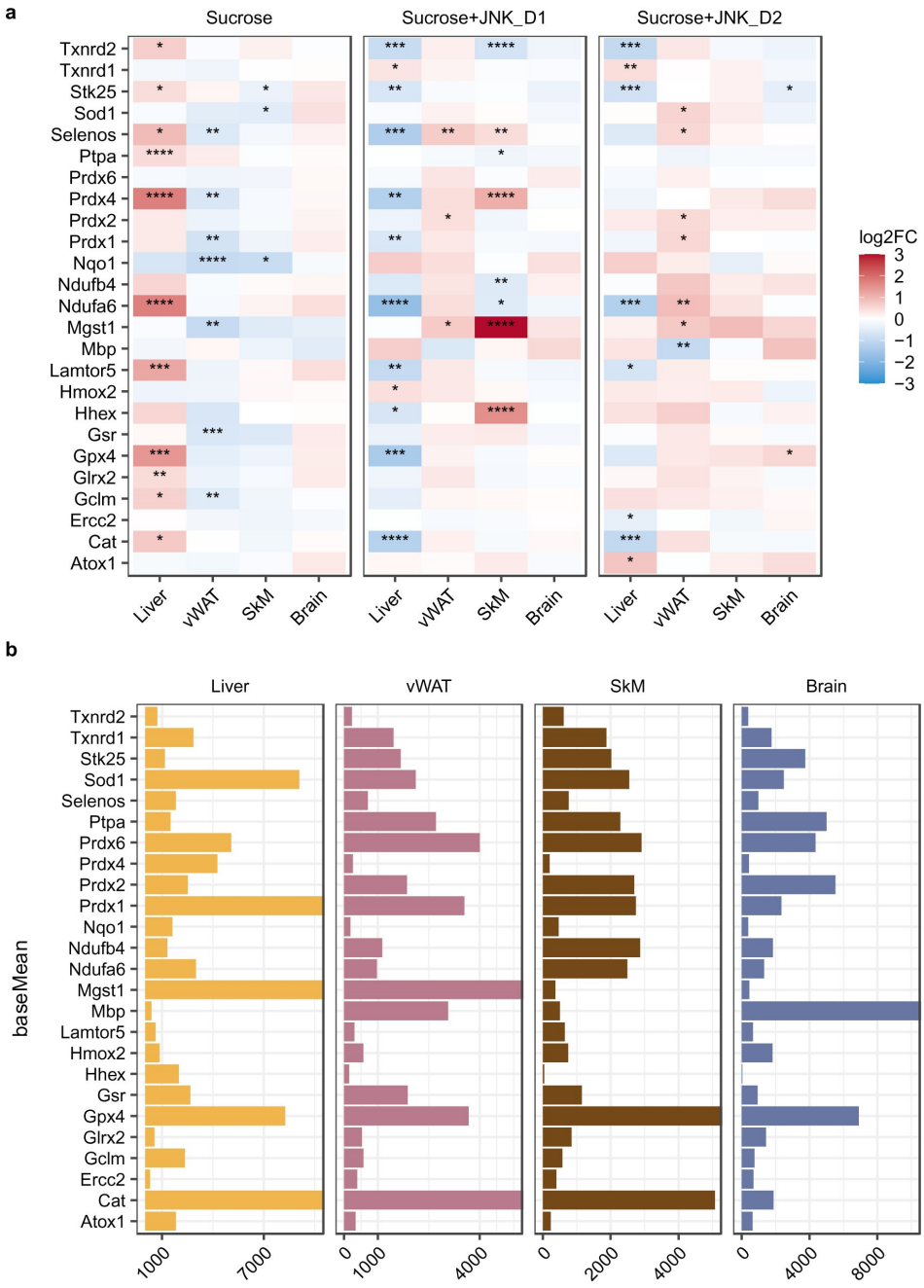

Figure S5.

Relative changes of genes involved in redox homeostasis in response to sucrose consumption and JNK-in-5A treatment in the tissues, related to **Fig. 2**.

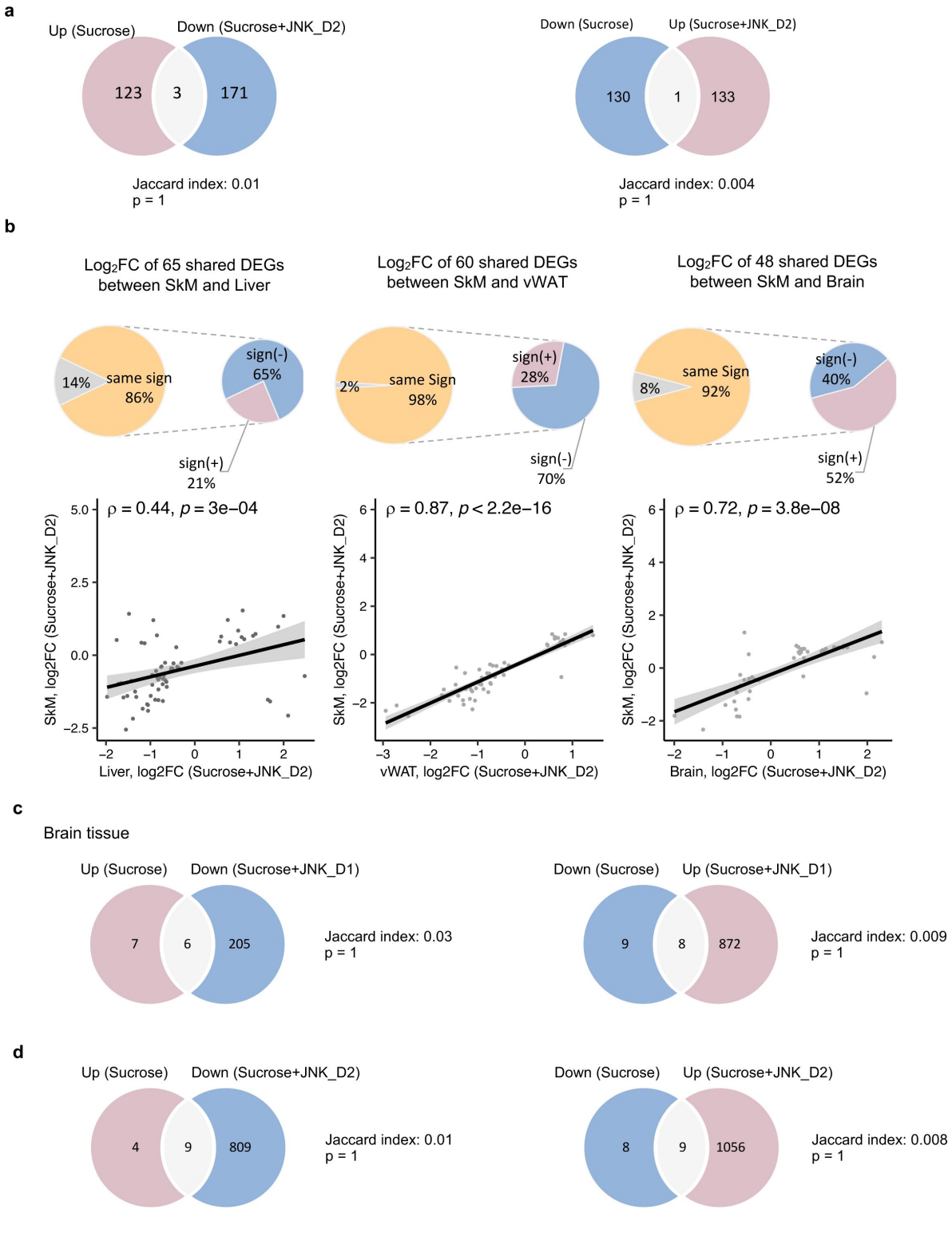

Figure S6.

(**a**) Venn diagram showing the overlap between significantly regulated genes response to sucrose consumption and JNK_D2 treatment in SkM, see also **Fig. S1** &**Fig. S5**. (**b**) Correlation of $\log_2$(Fold change) for shared DEGs between the SkM and Liver, vWAT, or Brain after JNK_D2 treatment. (c) Venn diagram showing the overlap between significantly regulated genes response to sucrose consumption and JNK_D1 treatment as well as (**d**) JNK_D2 treatment in the Brain, respectively.

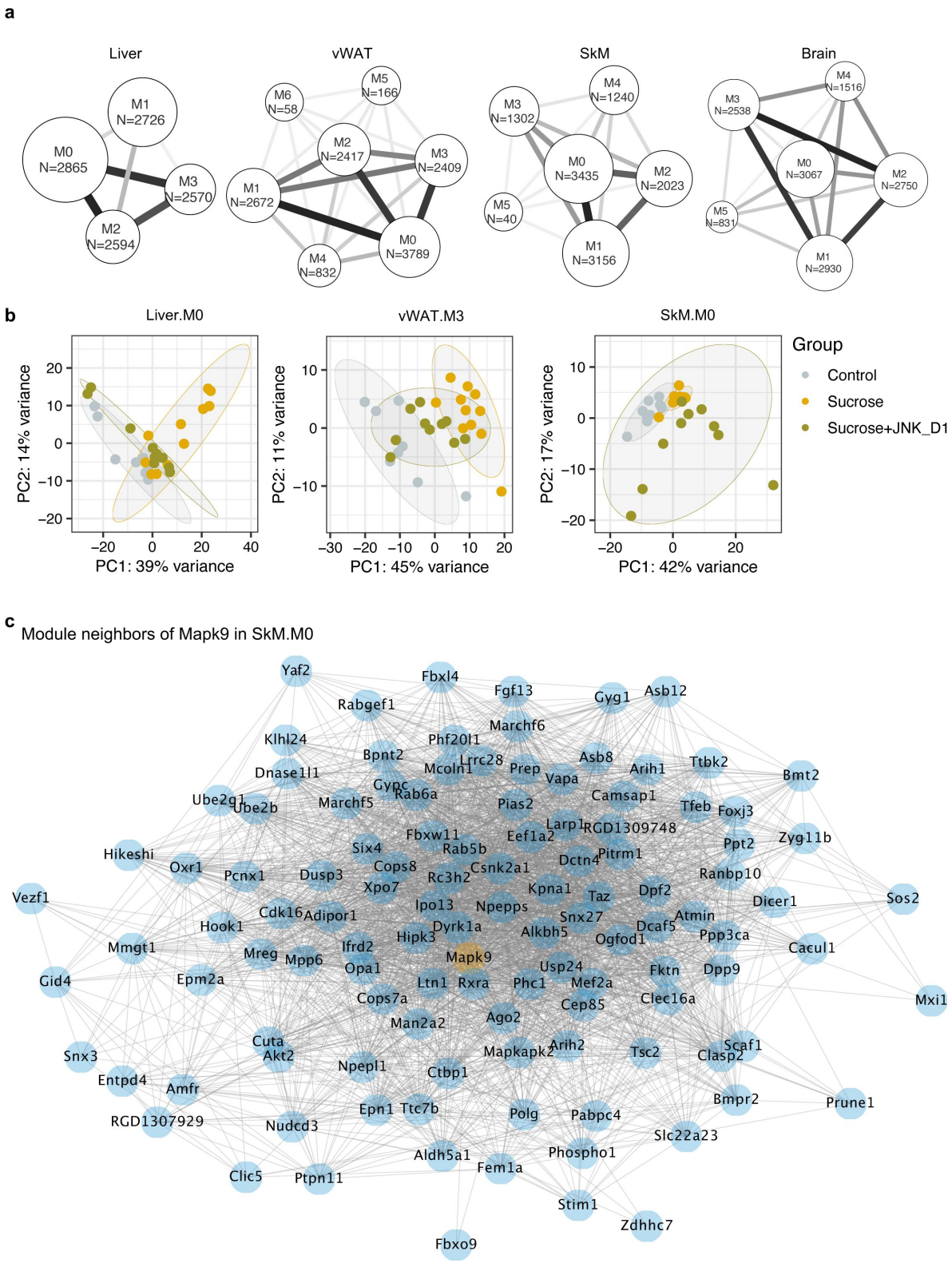

Figure S7.

(**a**) The number of gene modules are identified from the tissue-specific co-expression networks. The text on the module indicates the module name and the number of genes of individual modules in each tissue. The edges between the clusters were aggregations of the inter-cluster edges. (**b**) PCA of Liver.M0, vWAT.M3, and SkM.M0 gene expression data. (**c**) Module neighbors of Mapk9 in SkM.M0.

Data Availability

All raw RNA-sequencing data generated from this study can be accessed through GEO accession number GSE282954.

Acknowledgements

The authors would like to acknowledge financial support from ScandiEdge Therapeutics and the Knut and Alice Wallenberg Foundation (No. 72110). A.M. and H.Y. acknowledge support from the PoLiMeR Innovative Training Network (Marie Skłodowska-Curie Grant Agreement No. 812616) which has received funding from the European Union's Horizon 2020 research and innovation program. The computations were performed on resources provided by SNIC through the Uppsala Multidisciplinary Center for Advanced Computational Science (UPPMAX) under Project sllstore2017024 and sctatlas.

Additional information

Author contributions

A.M. conceived and designed the analysis; M.K., C.B., I.B., O.O.T., C.B., N.Y., S.Y., S.I., J.S., A.H., H.T. collected data for the study; H.Y., C.Z., W.K., M.N.SH. performed the data analysis, visualization, and interpretation; H.Y. drat the manuscript; All authors read and approved the final manuscript.

Additional files

Data S1. *Summary of body weight and clinical pathological parameters for 7 days oral toxicology of JNK-IN-5A in rats.*

Data S2. *Summary of body weight and clinical pathological parameters for 3 weeks oral administration of JNK-IN-5A in MAFLD rats model.*

Data S3. *Passive avoidance data.*

Data S4. *Locomotor activity data.*

Data S5. *Elevated plus maze data.*

Data S6. *Result of differential expression analysis for all relevant comparisons of liver, white adipose tissue, skeletal muscle and brain in the study, related to Fig. 2-4.*

Data S7. *Gene membership in certain module identified from the tissue-specific co-expression networks, which includes samples from Control, Sucrose and Sucrose+JNK_D1 groups, related to Fig. 6.*

Data S8. *Results of genome-scale metabolic modelling based on Compass and Recon3D, related to Fig. 7.*

References

Angell R. M., Atkinson F. L., Brown M. J., Chuang T. T., Christopher J. A., Cichy-Knight M., Dunn A. K., Hightower K. E., Malkakorpi S., Musgrave J. R., Neu M., Rowland P., Shea R. L., Smith J. L., Somers D. O., Thomas S. A., Thompson G., Wang R 2007) **N-(3-Cyano-4,5,6,7-tetrahydro-1-benzothien-2-yl)amides as potent, selective, inhibitors of JNK2 and JNK3** *Bioorg Med Chem Lett* **17**:1296–301

Arif M., Klevstig M., Benfeitas R., Doran S., Turkez H., Uhlen M., Clausen M., Wikstrom J., Etal D., Zhang C., Levin M., Mardinoglu A., Boren J 2021) **Integrative transcriptomic analysis of tissue-specific metabolic crosstalk after myocardial infarction** *Elife* **10**

Azzu V., Vacca M., Virtue S., Allison M., Vidal-Puig A 2020) **Adipose Tissue-Liver Cross Talk in the Control of Whole-Body Metabolism: Implications in Nonalcoholic Fatty Liver Disease** *Gastroenterology* **158**:1899–1912

Barabasi A. L., Albert R 1999) **Emergence of scaling in random networks** *Science* **286**:509–12

Bray N. L., Pimentel H., Melsted P., Pachter L 2016) **Near-optimal probabilistic RNA-seq quantification** *Nat Biotechnol* **34**:525–7

Brunk E., Sahoo S., Zielinski D. C., Altunkaya A., Drager A., Mih N., Gatto F., Nilsson A., Preciat Gonzalez G. A., Aurich M. K., Prlic A., Sastry A., Danielsdottir A. D., Heinken A., Noronha A., Rose P. W., Burley S. K., Fleming R. M. T., Nielsen J., Thiele I., Palsson B. O 2018) **Recon3D enables a three-dimensional view of gene variation in human metabolism** *Nat Biotechnol* **36**:272–281

Califano A., Butte A. J., Friend S., Ideker T., Schadt E 2012) **Leveraging models of cell regulation and GWAS data in integrative network-based association studies** *Nat Genet* **44**:841–7

Cerbone A., Toaldo C., Pizzimenti S., Pettazzoni P., Dianzani C., Minelli R., Ciamporcero E., Roma G., Dianzani M. U., Canaparo R., Ferretti C., Barrera G 2012) **AS601245, an Anti-Inflammatory JNK Inhibitor, and Clofibrate Have a Synergistic Effect in Inducing Cell Responses and in Affecting the Gene Expression Profile in CaCo-2 Colon Cancer Cells** *PPAR Res* **2012**

Chang L., Karin M 2001) **Mammalian MAP kinase signalling cascades** *Nature* **410**:37–40

Chellian R., Behnood-Rod A., Wilson R., Wilks I., Knight P., Febo M., Bruijnzeel A. W. 2020) **Exposure to smoke from high- but not low-nicotine cigarettes leads to signs of dependence in male rats and potentiates the effects of nicotine in female rats** *Pharmacol Biochem Behav* **196**

Choobdar S., Ahsen M. E., Crawford J., Tomasoni M., Fang T., Lamparter D., Lin J., Hescott B., Hu X., Mercer J., Natoli T., Narayan R., Consortium D. M. I. C., Subramanian A., Zhang J. D., Stolovitzky G., Kutalik Z., Lage K., Slonim D. K., Saez-Rodriguez J., Cowen L. J., Bergmann S., Marbach D 2019) **Assessment of network module identification across complex diseases** *Nat Methods* **16**:843–852

Czaja M. J 2010) **JNK regulation of hepatic manifestations of the metabolic syndrome** *Trends Endocrinol Metab* **21**:707–13

Dobrin R., Zhu J., Molony C., Argman C., Parrish M. L., Carlson S., Allan M. F., Pomp D., Schadt E. E 2009) **Multi-tissue coexpression networks reveal unexpected subnetworks associated with disease** *Genome Biol* **10**

Eryavuz Onmaz D., Ozturk B. 2022) **Altered Kynurenine Pathway Metabolism in Rats Fed Added Sugars** *Genel Tıp Dergisi* **32**:525–529

Ferah Okkay I., Okkay U., Gundogdu O. L., Bayram C., Mendil A. S., Ertugrul M. S., Hacimuftuoglu A. 2022) **Syringic acid protects against thioacetamide-induced hepatic encephalopathy: Behavioral, biochemical, and molecular evidence** *Neurosci Lett* **769**

Geidl-Flueck B., Hochuli M., Nemeth A., Eberl A., Derron N., Kofeler H. C., Tappy L., Berneis K., Spinas G. A., Gerber P. A 2021) **Fructose- and sucrose- but not glucose-sweetened beverages promote hepatic de novo lipogenesis: A randomized controlled trial** *J Hepatol* **75**:46–54

Geurtsen M. L., Santos S., Gaillard R., Felix J. F., Jaddoe V. W. V 2021) **Associations Between Intake of Sugar-Containing Beverages in Infancy With Liver Fat Accumulation at School Age** *Hepatology* **73**:560–570

Gimenez De Bejar V., Caballero Bleda M., Popovic N., Popovic M. 2017) **Verapamil Blocks Scopolamine Enhancement Effect on Memory Consolidation in Passive Avoidance Task in Rats** *Front Pharmacol* **8**

Hosseini N., Alaei H., Reisi P., Radahmadi M 2013) **The effect of treadmill running on passive avoidance learning in animal model of Alzheimer disease** *Int J Prev Med* **4**:187–92

Jang C., Wada S., Yang S., Gosis B., Zeng X., Zhang Z., Shen Y., Lee G., Arany Z., Rabinowitz J. D 2020) **The small intestine shields the liver from fructose-induced steatosis** *Nat Metab* **2**:586–593

Jeon Y. G., Kim Y. Y., Lee G., Kim J. B 2023) **Physiological and pathological roles of lipogenesis** *Nat Metab* **5**:735–759

Kanehisa M 2002) **The KEGG database** *Novartis Found Symp* **247**:91–101

Karlsen T. H., Sheron N., Zelber-Sagi S., Carrieri P., Dusheiko G., Bugianesi E., Pryke R., Hutchinson S. J., Sangro B., Martin N. K., Cecchini M., Dirac M. A., Belloni A., Serra-Burriel M., Ponsioen C. Y., Sheena B., Lerouge A., Devaux M., Scott N., Hellard M., Verkade H. J., Sturm E., Marchesini G., Yki-Jarvinen H., Byrne C. D., Targher G., Tur-Sinai A., Barrett D., Ninburg M., Reic T., Taylor A., Rhodes T., Treloar C., Petersen C., Schramm C., Flisiak R., Simonova M. Y., Pares A., Johnson P., Cucchetti A., Graupera I., Lionis C., Pose E., Fabrellas N., Ma A. T., Mendive J. M., Mazzaferro V., Rutter H., Cortez-Pinto H., Kelly D., Burton R., Lazarus J. V., Gines P., Buti M., Newsome P. N., Burra P., Manns M. P 2022) **The EASL-Lancet Liver Commission: protecting the next generation of Europeans against liver disease complications and premature mortality** *Lancet* **399**:61–116

Kim W., Li M., Jin H., Yang H., Turkez H., Uhlen M., Zhang C., Mardinoglu A 2023) **Characterization of an in vitro steatosis model simulating activated de novo lipogenesis in MAFLD patients** *iScience* **26**

Kodama Y., Brenner D. A 2009) **. c-Jun N-terminal kinase signaling in the pathogenesis of nonalcoholic fatty liver disease: Multiple roles in multiple steps** *Hepatology* **49**:6–8

Kotsiliti E 2023) **NAFLD incidence is increasing** *Nat Rev Gastroenterol Hepatol* **20**

Lamb J. A., Ventura J. J., Hess P., Flavell R. A., Davis R. J 2003) **JunD mediates survival signaling by the JNK signal transduction pathway** *Mol Cell* **11**:1479–89

Le M. H., Le D. M., Baez T. C., Wu Y., Ito T., Lee E. Y., Lee K., Stave C. D., Henry L., Barnett S. D., Cheung R., Nguyen M. H 2023) **Global incidence of non-alcoholic fatty liver disease: A systematic review and meta-analysis of 63 studies and 1,201,807 persons** *J Hepatol* **79**:287–295

Lessard S. J., MacDonald T. L., Pathak P., Han M. S., Coffey V. G., Edge J., Rivas D. A., Hirshman M. F., Davis R. J., Goodyear L. J 2018) **JNK regulates muscle remodeling via myostatin/SMAD inhibition** *Nat Commun* **9**

Liberzon A., Birger C., Thorvaldsdottir H., Ghandi M., Mesirov J. P., Tamayo P 2015) **The Molecular Signatures Database (MSigDB) hallmark gene set collection** *Cell Syst* **1**:417–425

Llovet J. M., Willoughby C. E., Singal A. G., Greten T. F., Heikenwalder M., El-Serag H. B., Finn R. S., Friedman S. L 2023) **Nonalcoholic steatohepatitis-related hepatocellular carcinoma: pathogenesis and treatment** *Nat Rev Gastroenterol Hepatol* **20**:487–503

Love M. I., Huber W., Anders S 2014) **Moderated estimation of fold change and dispersion for RNA-seq data with DESeq2** *Genome Biol* **15**

Lu Y., Sareddy G. R., Wang J., Wang R., Li Y., Dong Y., Zhang Q., Liu J., O'Connor J. C., Xu J., Vadlamudi R. K., Brann D. W 2019) **Neuron-Derived Estrogen Regulates Synaptic Plasticity and Memory** *J Neurosci* **39**:2792–2809

Machado M. V., Cortez-Pinto H 2023) **NAFLD, MAFLD and obesity: brothers in arms?** *Nat Rev Gastroenterol Hepatol* **20**:67–68

Malik V. S., Hu F. B 2022) **The role of sugar-sweetened beverages in the global epidemics of obesity and chronic diseases** *Nat Rev Endocrinol* **18**:205–218

Mardinoglu A., Agren R., Kampf C., Asplund A., Nookaew I., Jacobson P., Walley A. J., Froguel P., Carlsson L. M., Uhlen M., Nielsen J 2013) **Integration of clinical data with a genome-scale metabolic model of the human adipocyte** *Mol Syst Biol* **9**

Mardinoglu A., Boren J., Smith U., Uhlen M., Nielsen J 2018) **Systems biology in hepatology: approaches and applications** *Nat Rev Gastroenterol Hepatol* **15**:365–377

Mardinoglu A., Nielsen J. 2012) **Systems medicine and metabolic modelling** *J Intern Med* **271**:142–54

Mardinoglu A., Palsson B. O 2024) **Genome-scale models in human metabologenomics** *Nat Rev Genet*

Martin F. J., Amode M. R., Aneja A., Austine-Orimoloye O., Azov A. G., Barnes I., Becker A., Bennett R., Berry A., Bhai J., Bhurji S. K., Bignell A., Boddu S., Branco Lins P. R., Brooks L., Ramaraju S. B., Charkhchi M., Cockburn A., Da Rin Fiorretto L., Davidson C., Dodiya K., Donaldson S., El Houdaigui B., El Naboulsi T., Fatima R., Giron C. G., Genez T., Ghattaoraya G. S., Martinez J. G., Guijarro C., Hardy M., Hollis Z., Hourlier T., Hunt T., Kay M., Kaykala V., Le T., Lemos D., Marques-Coelho D., Marugan J. C., Merino G. A., Mirabueno L. P., Mushtaq A., Hossain S. N., Ogeh D. N., Sakthivel M. P., Parker A., Perry M., Pilizota I., Prosovetskaia I., Perez-

Silva J. G., Salam A. I. A., Saraiva-Agostinho N., Schuilenburg H., Sheppard D., Sinha S., Sipos B., Stark W., Steed E., Sukumaran R., Sumathipala D., Suner M. M., Surapaneni L., Sutinen K., Szpak M., Tricomi F. F., Urbina-Gomez D., Veidenberg A., Walsh T. A., Walts B., Wass E., Willhoft N., Allen J., Alvarez-Jarreta J., Chakiachvili M., Flint B., Giorgetti S., Haggerty L., Ilsley G. R., Loveland J. E., Moore B., Mudge J. M., Tate J., Thybert D., Trevanion S. J., Winterbottom A., Frankish A., Hunt S. E., Ruffier M., Cunningham F., Dyer S., Finn R. D., Howe K. L., Harrison P. W., Yates A. D., Flicek P 2023) **Ensembl 2023** *Nucleic Acids Res* **51**:D933–D941

Nassir F., Rector R. S., Hammoud G. M., Ibdah J. A 2015) **Pathogenesis and Prevention of Hepatic Steatosis** *Gastroenterol Hepatol (N Y)* **11**:167–75

Nikolic I., Leiva M., Sabio G 2020) **The role of stress kinases in metabolic disease** *Nat Rev Endocrinol* **16**:697–716

Orth J. D., Thiele I., Palsson B. O 2010) **What is flux balance analysis?** *Nat Biotechnol* **28**:245–8

Papa S., Bubici C 2018) **Feeding the Hedgehog: A new meaning for JNK signalling in liver regeneration** *J Hepatol* **69**:572–574

Sabio G., Cavanagh-Kyros J., Ko H. J., Jung D. Y., Gray S., Jun J. Y., Barrett T., Mora A., Kim J. K., Davis R. J 2009) **Prevention of steatosis by hepatic JNK1** *Cell Metab* **10**:491–8

Sabio G., Davis R. J 2010) **cJun NH2-terminal kinase 1 (JNK1): roles in metabolic regulation of insulin resistance** *Trends Biochem Sci* **35**:490–6

Schattenberg J. M., Singh R., Wang Y., Lefkowitch J. H., Rigoli R. M., Scherer P. E., Czaja M. J 2006) **JNK1 but not JNK2 promotes the development of steatohepatitis in mice** *Hepatology* **43**:163–72

Seki E., Brenner D. A., Karin M 2012) **A liver full of JNK: signaling in regulation of cell function and disease pathogenesis, and clinical approaches** *Gastroenterology* **143**:307–20

Singh R., Wang Y., Xiang Y., Tanaka K. E., Gaarde W. A., Czaja M. J 2009) **Differential effects of JNK1 and JNK2 inhibition on murine steatohepatitis and insulin resistance** *Hepatology* **49**:87–96

Softic S., Stanhope K. L., Boucher J., Divanovic S., Lanaspa M. A., Johnson R. J., Kahn C. R 2020) **Fructose and hepatic insulin resistance** *Crit Rev Clin Lab Sci* **57**:308–322

Solinas G., Becattini B 2017) **JNK at the crossroad of obesity, insulin resistance, and cell stress response** *Mol Metab* **6**:174–184

Soneson C., Love M. I., Robinson M. D 2015) **Differential analyses for RNA-seq: transcript-level estimates improve gene-level inferences** *F1000Res* **4**

Sousa R. M. L., Ribeiro N. L. X., Pinto B. A. S., Sanches J. R., da Silva M. U., Coelho C. F. F., Franca L. M., de Figueiredo Neto J. A., Paes A. M. A. 2018) **Long-term high-protein diet intake reverts weight gain and attenuates metabolic dysfunction on high-sucrose-fed adult rats** *Nutr Metab (Lond* **15**

Stephenson E. J., Stayton A. S., Sethuraman A., Rao P. K., Meyer A., Gomes C. K., Mulcahy M. C., McAllan L., Puchowicz M. A., Pierre J. F., Bridges D., Han J. C 2022) **Chronic intake of high dietary sucrose induces sexually dimorphic metabolic adaptations in mouse liver and adipose tissue** *Nat Commun* **13**

Sveinbjornsson G., Ulfarsson M. O., Thorolfsdottir R. B., Jonsson B. A., Einarsson E., Gunnlaugsson G., Rognvaldsson S., Arnar D. O., Baldvinsson M., Bjarnason R. G., consortium D. G., Eiriksdottir T., Erikstrup C., Ferkingstad E., Halldorsson G. H., Helgason H., Helgadottir A., Hindhede L., Hjorleifsson G., Jones D., Knowlton K. U., Lund S. H., Melsted P., Norland K., Olafsson I., Olafsson S., Oskarsson G. R., Ostrowski S. R., Pedersen O. B., Snaebjarnarson A. S., Sigurdsson E., Steinthorsdottir V., Schwinn M., Thorgeirsson G., Thorleifsson G., Jonsdottir I., Bundgaard H., Nadauld L., Bjornsson E. S., Rulifson I. C., Rafnar T., Norddahl G. L., Thorsteinsdottir U., Sulem P., Gudbjartsson D. F., Holm H., Stefansson K. 2022) **Multiomics study of nonalcoholic fatty liver disease** *Nat Genet* **54**:1652–1663

Traag V. A., Waltman L., van Eck N. J. 2019) **From Louvain to Leiden: guaranteeing well-connected communities** *Sci Rep* **9**

Vernia S., Cavanagh-Kyros J., Garcia-Haro L., Sabio G., Barrett T., Jung D. Y., Kim J. K., Xu J., Shulha H. P., Garber M., Gao G., Davis R. J 2014) **The PPARalpha-FGF21 hormone axis contributes to metabolic regulation by the hepatic JNK signaling pathway** *Cell Metab* **20**:512–25

Virtanen P., Gommers R., Oliphant T. E., Haberland M., Reddy T., Cournapeau D., Burovski E., Peterson P., Weckesser W., Bright J., van der Walt S. J., Brett M., Wilson J., Millman K. J., Mayorov N., Nelson A. R. J., Jones E., Kern R., Larson E., Carey C. J., Polat I., Feng Y., Moore E. W., VanderPlas J., Laxalde D., Perktold J., Cimrman R., Henriksen I., Quintero E. A., Harris C. R., Archibald A. M., Ribeiro A. H., Pedregosa F., van Mulbregt P., SciPy C. 2020) **SciPy 1.0: fundamental algorithms for scientific computing in Python** *Nat Methods* **17**:261–272

Wagner A., Wang C., Fessler J., DeTomaso D., Avila-Pacheco J., Kaminski J., Zaghouani S., Christian E., Thakore P., Schellhaass B., Akama-Garren E., Pierce K., Singh V., Ron-Harel N., Douglas V. P., Bod L., Schnell A., Puleston D., Sobel R. A., Haigis M., Pearce E. L., Soleimani M., Clish C., Regev A., Kuchroo V. K., Yosef N. 2021) **Metabolic modeling of single Th17 cells reveals regulators of autoimmunity** *Cell* **184**:4168–4185

Walf A. A., Frye C. A 2007) **The use of the elevated plus maze as an assay of anxiety-related behavior in rodents** *Nat Protoc* **2**:322–8

Wu C., Yang L., Li Y., Dong Y., Yang B., Tucker L. D., Zong X., Zhang Q 2020) **Effects of Exercise Training on Anxious-Depressive-like Behavior in Alzheimer Rat** *Med Sci Sports Exerc* **52**:1456–1469

Xiao X., Lai W., Xie H., Liu Y., Guo W., Liu Y., Li Y., Li Y., Zhang J., Chen W., Shi M., Shang L., Yin M., Wang C., Deng H 2019) **Targeting JNK pathway promotes human hematopoietic stem cell expansion** *Cell Discov* **5**

Yang H., Arif M., Yuan M., Li X., Shong K., Turkez H., Nielsen J., Uhlen M., Boren J., Zhang C., Mardinoglu A 2021) **A network-based approach reveals the dysregulated transcriptional regulation in non-alcoholic fatty liver disease** *iScience* **24**

Yang Y., Han L., Yuan Y., Li J., Hei N., Liang H 2014) **Gene co-expression network analysis reveals common system-level properties of prognostic genes across cancer types** *Nat Commun* **5**

Yki-Jarvinen H., Luukkonen P. K., Hodson L., Moore J. B 2021) **Dietary carbohydrates and fats in nonalcoholic fatty liver disease** *Nat Rev Gastroenterol Hepatol* **18**:770–786

Younossi Z. M., Golabi P., Paik J. M., Henry A., Van Dongen C., Henry L. 2023) **The global epidemiology of nonalcoholic fatty liver disease (NAFLD) and nonalcoholic steatohepatitis (NASH): a systematic review** *Hepatology* **77**:1335–1347

Zhang C., Lee S., Mardinoglu A., Hua Q 2016) **Investigating the Combinatory Effects of Biological Networks on Gene Co-expression** *Front Physiol* **7**

Zhang S., Gu Y., Bian S., Lu Z., Zhang Q., Liu L., Meng G., Yao Z., Wu H., Wang Y., Zhang T., Wang X., Sun S., Wang X., Zhou M., Jia Q., Song K., Qi L., Niu K 2021) **Soft drink consumption and risk of nonalcoholic fatty liver disease: results from the Tianjin Chronic Low-Grade Systemic Inflammation and Health (TCLSIH) cohort study** *Am J Clin Nutr* **113**:1265–1274

Author information

Hong Yang
Science for Life Laboratory, KTH - Royal Institute of Technology, Stockholm, Sweden

Cheng Zhang
Science for Life Laboratory, KTH - Royal Institute of Technology, Stockholm, Sweden
ORCID iD: 0000-0002-3721-8586

Woonghee Kim
Science for Life Laboratory, KTH - Royal Institute of Technology, Stockholm, Sweden

Mengnan Shi
Science for Life Laboratory, KTH - Royal Institute of Technology, Stockholm, Sweden

Metin Kiliclioglu
Department of Pathology, Veterinary Faculty, Atatürk University, Erzurum, Turkiye

Cemil Bayram
Department of Medical Pharmacology, Faculty of Medicine, Atatürk University, Erzurum, Turkiye

Ismail Bolat
Department of Pathology, Veterinary Faculty, Atatürk University, Erzurum, Turkiye

Özlem Özdemir Tozlu
Department of Molecular Biology and Genetics, Faculty of Science, Erzurum Technical University, Erzurum, Turkiye

Cem Baba
Department of Molecular Biology and Genetics, Faculty of Science, Erzurum Technical University, Erzurum, Turkiye

Nursena Yuksel
Department of Molecular Biology and Genetics, Faculty of Science, Erzurum Technical University, Erzurum, Turkiye

Serkan Yildirim
Department of Pathology, Veterinary Faculty, Atatürk University, Erzurum, Turkiye

Shazia Iqbal
Trustlife Labs Drug Research & Development Center, Istanbul, Turkiye

Jihad Sebhaoui
Trustlife Labs Drug Research & Development Center, Istanbul, Turkiye

Ahmet Hacımuftuoglu
Department of Medical Pharmacology, Faculty of Medicine, Atatürk University, Erzurum, Turkiye

Mathias Uhlen
Science for Life Laboratory, KTH - Royal Institute of Technology, Stockholm, Sweden
ORCID iD: 0000-0002-4858-8056

Jan Boren
Department of Molecular and Clinical Medicine, University of Gothenburg, Sahlgrenska University Hospital, Gothenburg, Sweden

Hasan Turkez
Department of Medical Biology, Faculty of Medicine, Atatürk University, Erzurum, Turkiye

Adil Mardinoglu
Science for Life Laboratory, KTH - Royal Institute of Technology, Stockholm, Sweden, Centre for Host-Microbiome Interactions, Faculty of Dentistry, Oral & Craniofacial Sciences, King's College London, London, United Kingdom

For correspondence: adilm@scilifelab.se

Editors

Reviewing Editor
Marcus Seldin
University of California, Irvine, Irvine, United States of America

Senior Editor
David James
University of Sydney, Sydney, Australia

Reviewer #1 (Public review):

Summary:

In this manuscript, authors have investigated the effects of JNK inhibition on sucrose-induced metabolic dysfunction in rats. They used multi-tissue network analysis to study the effects of the JNK inhibitor JNK-IN-5A on metabolic dysfunction associated with excessive sucrose consumption. Their results show that JNK inhibition reduces triglyceride accumulation and inflammation in the liver and adipose tissues while promoting metabolic adaptations in skeletal muscle. The study provides new insights into how JNK inhibition can potentially treat

metabolic dysfunction-associated fatty liver disease (MAFLD) by modulating inter-tissue communication and metabolic processes.

Strengths:

The study has several notable strengths:

Comprehensive Multi-Tissue Analysis: The research provides a thorough multi-tissue evaluation, examining the effects of JNK inhibition across key metabolically active tissues, including the liver, visceral white adipose tissue, skeletal muscle, and brain. This comprehensive approach offers valuable insights into the systemic effects of JNK inhibition and its potential in treating MAFLD.

Robust Use of Systems Biology: The study employs advanced systems biology techniques, including transcriptomic analysis and genome-scale metabolic modeling, to uncover the molecular mechanisms underlying JNK inhibition. This integrative approach strengthens the evidence supporting the role of JNK inhibitors in modulating metabolic pathways linked to MAFLD.

Potential Therapeutic Insights: By demonstrating the effects of JNK inhibition on both hepatic and extrahepatic tissues, the study offers promising therapeutic insights into how JNK inhibitors could be used to mitigate metabolic dysfunction associated with excessive sucrose consumption, a key contributor to MAFLD.

Behavioral and Metabolic Correlation: The inclusion of behavioral tests alongside metabolic assessments provides a more holistic view of the treatment's effects, allowing for a better understanding of the broader physiological implications of JNK inhibition.

Weaknesses:

The authors have adequately addressed all my concerns, and the revisions have significantly improved the manuscript's clarity and impact.

https://doi.org/10.7554/eLife.98427.2.sa2

Reviewer #2 (Public review):

Excessive sucrose is a possible initial factor for the development of metabolic dysfunction-associated fatty liver disease (MAFLD). To investigate the possibility that intervention with JNK inhibitor could lead to the treatment of metabolic dysfunction caused by excessive sucrose intake, the authors performed multi-organ transcriptomics analysis (liver, visceral fat (vWAT), skeletal muscle, and brain) in a rat model of MAFLD induced by sucrose overtake (+ JNK inhibitor treatment).

The major strengths and weakness of this study are as follows.

Strengths:

・It has been previously reported that inhibition of JNK signalling can contribute to the prevention of hepatic steatosis (HS) and related metabolic syndrome in other models, but the role of JNK signalling in the metabolic disruption caused by excessive intake of sucrose, a possible initial factor for the development of MAFLD, has not been well understood, and the authors have addressed this point.
・This study is also important because pharmacological therapy for MAFLD has not yet been established.
・By obtaining transcriptomic data in multiple organs and comprehensively analyzing the data using gene co-expression network (GCN) analysis and genome-scale metabolic models

(GEM), the authors showed the multi-organ interaction in not only in the pathology of MAFLD caused by excessive sucrose intake but also in the treatment effects by JNK-IN-5A.
・Since JNK signalling has diverse physiological functions in many organs, the authors effectively assessed possible side effects with a view to the clinical application of JNK-IN-5A.

Weaknesses:

・The metabolic process activities were evaluated using RNA-seq results in Figure 7, but direct data such as metabolite measurements are lacking.
・There is a lack of consistency in the data between JNK-IN-5A_D1 and _D2, and there is no sufficient data-based explanation for why the effects observed in D1 were inconsistent in the D2 samples.
・Although it is valuable that the authors were able to suggest the possibility of JNK inhibitor as a therapeutic strategy for MAFLD, the evaluation of the therapeutic effect was limited to evaluation of plasma TG, LDH, and gene expression changes. As there was no evaluation of liver tissue images, it is unclear what changes were brought about in the liver by the excessive sucrose intake and the treatment with JNK-IN-5A.

As mentioned in the Weakness section, biological data is insufficient, such as the lack of metabolite measurements and a histological evaluation of the liver. However, overall, the authors successfully provided the valuable insights that the JNK inhibitor has a cross-organ therapeutic effect on their MAFLD model induced by sucrose overtake. Their insist is supported by convincing data, comprehensively analysing the transcriptomic data obtained from multiple organs using GCN (gene co-expression network) analysis and GEM (genome-scale metabolic modelling).

Their comprehensive transcriptomic analysis in multiple organs, including the brain, has demonstrated that the effects of drugs are more widespread than just on specific tissues thought to be the main target, indicating the importance of focusing on tissue interactions when we assess the effects of drugs. Also, the data set in this study will be useful for comparative evaluation with transcriptomics data for other MALFD models.

https://doi.org/10.7554/eLife.98427.2.sa1

Author response:

The following is the authors' response to the original reviews.

> ***Public Reviews:***
>
> ***Reviewer #1 (Public review):***
>
> *Summary:*
>
> *In this manuscript, authors have investigated the effects of JNK inhibition on sucrose-induced metabolic dysfunction in rats. They used multi-tissue network analysis to study the effects of the JNK inhibitor JNK-IN-5A on metabolic dysfunction associated with excessive sucrose consumption. Their results show that JNK inhibition reduces triglyceride accumulation and inflammation in the liver and adipose tissues while promoting metabolic adaptations in skeletal muscle. The study provides new insights into how JNK inhibition can potentially treat metabolic dysfunction-associated fatty liver disease (MAFLD) by modulating inter-tissue communication and metabolic processes.*
>
> *Strengths:*
>
> *The study has several notable strengths:*

Comprehensive Multi-Tissue Analysis: The research provides a thorough multi-tissue evaluation, examining the effects of JNK inhibition across key metabolically active tissues, including the liver, visceral white adipose tissue, skeletal muscle, and brain. This comprehensive approach offers valuable insights into the systemic effects of JNK inhibition and its potential in treating MAFLD.

Robust Use of Systems Biology: The study employs advanced systems biology techniques, including transcriptomic analysis and genome-scale metabolic modeling, to uncover the molecular mechanisms underlying JNK inhibition. This integrative approach strengthens the evidence supporting the role of JNK inhibitors in modulating metabolic pathways linked to MAFLD.

Potential Therapeutic Insights: By demonstrating the effects of JNK inhibition on both hepatic and extrahepatic tissues, the study offers promising therapeutic insights into how JNK inhibitors could be used to mitigate metabolic dysfunction associated with excessive sucrose Behavioral and Metabolic Correlation: The inclusion of behavioral tests alongside metabolic assessments provides a more holistic view of the treatment's effects, allowing for a better understanding of the broader physiological implications of JNK inhibition.

Weaknesses:

While the study provides a comprehensive evaluation of JNK inhibitors in mitigating MAFLD conditions, addressing the following points will enhance the manuscript's quality:

The authors should explicitly mention and provide a detailed list of metabolites affected by sucrose and JNK inhibition treatment that have been previously associated with MAFLD conditions. This will better contextualize the findings within the broader field of metabolic disease research.

We fully agreed on this constructive suggestion to improve our understanding of the metabolic effect of JNK inhibition under sucrose overconsumption. While technical limitations made it challenging to directly analyze metabolites in the current study, we employed genome-scale metabolic modeling—a robust approach for studying metabolism—to predict the metabolic pathways potentially impacted by the interventions (Fig. 7 and Data S8). Additionally, as part of this revision, we conducted an extensive literature review to identify metabolites previously reported to be affected by sucrose consumption in MAFLD rodent models and MASLD patients. A detailed summary of these metabolites is now presented in attached Table 1 and several of these metabolites have been incorporated into the revised results section (Lines 308-314) to support some of the predicted metabolic activities.

“Some of the predicted metabolic changes align with previous findings in rodents subjected to sucrose overconsumption. For example, Öztürk et al. reported altered tryptophan metabolism, including decreased serum levels of kynurenic acid and kynurenine, in rats consuming 10% sucrose in drinking water. Similarly, increased triglyceride-bound oleate, palmitate, and stearate were observed in the livers of rats fed a 10% sucrose solution, indicating JNK-IN-5A treatment may regulate lipid metabolism by modulating these metabolic activities.”

It is important to note, however, that data on metabolites specifically affected by JNK inhibition in MASLD contexts remains lacking in the literature. The predicted metabolites and associated metabolic pathways in the current study could provide a starting point for such exploration in future studies. We have emphasized this in the revised manuscript and highlighted the need for further studies to explore these mechanisms in greater detail.

Author response table 1.

Metabolites associated with sucrose overconsumption in MASLD.

Study	Intervention(s) and duration	Metabolites	Metabolism
Fujii et al., 2024 [1].	Male rats fed a 10% sucrose solution for 16 days	Decreased blood acetate and butyrate levels	Gut microbial metabolism, Lipid metabolism
Sun et al., 2021 [2].	Male Wistar rats fed high-sucrose diet for 4 weeks	Decreased butyrate and formate in the cecal content	
Song et al., 2024 [3].	Male Wistar rats fed a high sucrose diet for 4 weeks	Decreased acetate and butyrate; increased succinate in cecal content	
Ramos-Romero et al., 2019 [4].	Male Wistar rats were fed a 35% sucrose solution for 24 weeks.	Increased uric acid in urine	Urea cycle
Ortiz & Field, 2023 [5].	Male C57BL/6J mice were fed either low-fat diet or high-fat diet with 30% sucrose water for 8 weeks	Elevated serum and kidney erythritol concentration	Carbohydrate metabolism
Beckmann et al. 2015 [6].	Healthy females (n=90) consumed 0, 50, or 100g sucrose in water, followed by urine and blood sampling at 0, 3, and 24 hours.	Increased erythronic acid in plasma	Carbohydrate metabolism
He et al., 2023 [7].	Male C57BL/6J mice were fed a high sucrose diet (30% sucrose in drinking water) for 24 weeks	Decreased muricholic acid level in the liver, cecal and colon content. increased hyocholic acid levels in the serum.	Bile acid metabolism
Stephenson et al. 2022 [8].	Mice fed 10% sucrose solution in drinking water for 12 weeks	Increased triglyceridebound oleate, palmitate, and stearate in liver; Mixed alteration in serum bile acids pool (sex and treatment interaction effect)	Lipid metabolism and bile acid metabolism
Mock et al. 2017 [9].	Female rats fed 13% sucrose solutions for 8 weeks	Increased palmitoleic acid in gonadal and retroperitoneal fat pads; higher serum triglyceride	Lipid metabolism
Oztürk et al. 2022 [10].	Wistar male rats fed 10% sucrose in drinking for 3 months	Decreased serum levels of kynurenic acid and kynurenine	Tryptophan metabolism
Gariani, Karim, et al. 2016 [11].	Male C57BL/6J mice were fed with a Western high-fat and highsucrose	Decreased NAD^+ levels in the liver	Fatty acid oxidation
Togo et al., 2019 [12].	C57BL/6J mice fed liquid (50% by weigh) or solid sucrose for 8 weeks	Elevated hepatic fat	Lipid metabolism

> *The limitations of the study should be clearly stated, particularly the lack of evidence on the effects of chronic JNK inhibitor treatment and potential off-target effects. Addressing these concerns will offer a more balanced perspective on the therapeutic potential of JNK inhibition.*

Thank you for this constructive comment. We have acknowledged limitations of the current study in Discussion section (Lines 397-406) of the revised manuscript:

“Nevertheless, several limitations warrant consideration. First, while we observed transcriptional adaptations in skeletal muscle tissue following treatment, the exact molecular mechanisms underlying these changes and their roles in skeletal muscle function and systemic metabolic homeostasis remain unclear. Further investigation is warranted to elucidate the muscle-specific effects of JNK inhibition. Second, our study did not investigate the dosedependent or potential off-target effects of JNK-IN-5A, particularly its activity on other members of the kinase family and associated signaling pathways. Lastly, the long-term effects of JNKIN-5A administration remain unexplored. Understanding its prolonged impact across different stages of MAFLD, including advanced MASH, is crucial for assessing the full therapeutic potential of JNK inhibition in the treatment of MAFLD.“

> *The potential risks of using JNK inhibitors in non-MAFLD conditions should be highlighted, with a clear distinction made between the preventive and curative effects of these therapies in mitigating MAFLD conditions. This will ensure the therapeutic implications are properly framed.*

Thank you for this insightful suggestion. The potential risks of using JNK inhibitors in nonMAFLD conditions have been considered and are now highlighted in Lines 369-390 of the revised discussion

“Although overactivated JNK activity presents an attractive opportunity to combat MAFLD, inhibition of JNK presents substantial challenges and potential risks due to its broad and multifaceted roles in many cellular processes. One key challenge is the dual role of JNK signaling (Lamb et al., 2003). For instance, long-term JNK inhibition may disrupt liver regeneration, as JNK plays a critical role in liver repair by regulating hepatocyte proliferation and survival following injury or stress (Papa and Bubici, 2018). In HCC, it has been reported that JNK acts as both a tumor promoter, driving inflammation, fibrosis, and metabolic dysregulation, and a tumor suppressor, facilitating apoptosis and cell cycle arrest in damaged hepatocytes. Its inhibition, therefore, carries the risk of inadvertently promoting tumor progression under certain conditions (Seki et al., 2012). Furthermore, the differential roles of JNK isoforms (JNK1, JNK2, JNK3) and a lack of specificity of JNK inhibitors present another layer of complexity. Given these challenges, while our study demonstrated the potential of JNK-IN-5A in mitigating early metabolic dysfunction in the liver and adipose tissues, JNK targeting strategies should be carefully tailored to the disease stage under investigation. For curative approaches targeting advanced MAFLD, such as MASH, future studies are warranted to address considerations related to dosing, tissue specificity, and the long-term effects.”

> *The statistical analysis section could be strengthened by providing a justification for the chosen statistical tests and discussing the study's power. Additionally, a more detailed breakdown of the behavioral test results and their implications would be beneficial for the overall conclusions of the study.*

We would like to thank you for this constructive suggestion. In this study, differences among more than two groups were tested using ANOVA or Kruskal-Wallis test based on the normality testing (Shapiro–Wilk test) on the data (continuous variables from different measurements). Pairwise comparisons, were performed using Tukey’s post hoc test following ANOVA or Dunn’s multiple comparisons post hoc test following the Kruskal-Wallis test, as appropriate.

The study used 11 animals per group, a group size widely used in preclinical animal research [13]. To evaluate the power of this study design to detect group differences, we conducted a

power analysis using G*Power 3.1 software [14], with ANOVA used as an example. The power analysis revealed the following:

- For a small effect size (partial eta.sq = 0.01), the power was 7.5% at p<0.05.

- For a medium effect size (partial eta.sq = 0.06), the power was 23.7% at p<0.05.

- For a large effect size (partial eta.sq = 0.14), the power is 55.4% at p<0.05

Bonapersona et al. reported that the median statistical power in animal studies is often between 15–22% [15], the achieved power of the current study design is within the range observed in most exploratory animal research. However, we acknowledge that the power for detecting smaller effects within groups is limited, which is also a common challenge in animal research due to ethical considerations on increasing sample sizes.

As suggested, we've revised the 'Statistical Analysis' and 'Result' sections to improve clarity:

"Statistical Analysis:

Data were shown as mean ± standard deviation (SD), unless stated otherwise. The assumption of normality for continuous variables from behavior test, biometric measurements, and plasm biochemistry was determined using the Shapiro–Wilk test. Differences among multiple groups were tested by ANOVA or, for data that were not normally distributed, the non-parametric Kruskal-Wallis test. Pairwise comparisons were performed using Tukey's post hoc test following the ANOVA or Dunn's multiple comparisons post hoc test following the Kruskal-Wallis test, as appropriate. The Jaccard index was used to evaluate the similarity and diversity of two gene sets, and a hypergeometric test was used to test the significance of their overlap. All results were considered statistically significant at p < 0.05, unless stated otherwise."

Behavior tests (Lines 150-157):

"We found no significant differences among groups in retention latencies, a measure of learning and memory abilities in passive avoidance test (Data S3). Additionally, the locomotor activity test was used to analyze behaviors such as locomotion, anxiety, and depression in rat. No significant differences were observed among groups in stereotypical movements, ambulatory activity, rearing, resting percentage, and distance travelled (Data S4). Similarly, the elevated plus maze test (Walf and Frye, 2007), an assay for assessing anxiety-like behavior in rodents, showed that rats in all groups had comparable open-arm entries and durations (Data S5). Collectively, the behavior tests indicate the JNK-IN-5A-treated rats exhibit no evidence of anxiety and behavior disorders."

> ***Reviewer #2 (Public review):***
>
> *Summary:*
>
> *Excessive sucrose is a possible initial factor for the development of metabolic dysfunctionassociated fatty liver disease (MAFLD). To investigate the possibility that intervention with JNK inhibitor could lead to the treatment of metabolic dysfunction caused by excessive sucrose intake, the authors performed multi-organ transcriptomics analysis (liver, visceral fat (vWAT), skeletal muscle, and brain) in a rat model of MAFLD induced by sucrose overtake (+ a selective JNK2 and JNK3 inhibitor (JNK-IN-5A) treatment). Their data suggested that changes in gene expression in the vWAT as well as in the liver contribute to the pathogenesis of their MAFLD model and revealed that the JNK inhibitor has a cross-organ therapeutic effect on it.*
>
> *Strengths:*

> *(1)It has been previously reported that inhibition of JNK signaling can contribute to the prevention of hepatic steatosis (HS) and related metabolic syndrome in other models, but the role of JNK signaling in the metabolic disruption caused by excessive intake of sucrose, a possible initial factor for the development of MAFLD, has not been well understood, and the authors have addressed this point.*
>
> *(2)This study is also important because pharmacological therapy for MAFLD has not yet been established.*
>
> *(3)By obtaining transcriptomic data in multiple organs and comprehensively analyzing the data using gene co-expression network (GCN) analysis and genome-scale metabolic models (GEM), the authors showed the multi-organ interaction in not only in the pathology of MAFLD caused by excessive sucrose intake but also in the treatment effects by JNK-IN-5A.*
>
> *(4) Since JNK signaling has diverse physiological functions in many organs, the authors effectively assessed possible side effects with a view to the clinical application of JNK-IN-5A.*
>
> *Weaknesses:*
>
> *(1) The metabolic process activities were evaluated using RNA-seq results in Figure 7, but direct data such as metabolite measurements are lacking.*

Thank you for these valuable insights. We fully agree that direct metabolite measurements would provide a deeper understanding of the metabolic impact of sucrose overconsumption and JNK-IN-5A administration. Unfortunately, due to technical limitations, we were unable to directly measure metabolites in this study. To address this, we supported our genome-scale metabolic modeling predictions with an extensive literature review, which is summarized in attached Table 1. This table highlights key metabolites and associated metabolic pathways that have been previously associated with sucrose overconsumption in MAFLD contexts. We incorporated some of these metabolites into the revised results section (Lines 308–314) to demonstrate the consistency between our predicted metabolic changes and experimental findings from the literature. For instance, studies have reported altered tryptophan metabolism, including decreased serum kynurenic acid and kynurenine levels, as well as increased triglyceride-bound oleate, palmitate, and stearate in sucrose-fed rodents. These findings align with our predictions of altered metabolic activities in fatty acid oxidation, fatty acid synthesis, and tryptophan metabolism.

> *(2) There is a lack of consistency in the data between JNK-IN-5A_D1 and _D2, and there is no sufficient data-based explanation for why the effects observed in D1 were inconsistent in the D2 samples.*

Thank you for raising this important point regarding the differences between the two dosages. As this was not the primary focus of the current study and we do not have sufficient data to fully explain these observations. Our speculation is that this may arise from pharmacokinetic differences associated with the dosing of this small molecule inhibitor, including potential saturation of transport mechanisms, alter tissue distribution, or off-target effects.

> *(3) Although it is valuable that the authors were able to suggest the possibility of JNK inhibitor as a therapeutic strategy for MAFLD, the evaluation of the therapeutic effect was limited to the evaluation of plasma TG, LDH, and gene expression changes. As there was no evaluation of liver tissue images, it is unclear what changes were brought about in the liver by the excessive sucrose intake and the treatment with JNK-IN-5A.*

We acknowledge that the lack of histological evaluations may limit to having a complete picture of the interventions' effects. However, as you noted, our transcriptional and systems-wide investigation across multiple tissues provides novel and significant insights into the molecular and systemic impacts of JNK-IN-5A treatment.

> ***Recommendations for the authors:***
>
> ***Reviewer #2 (Recommendations for the authors):***
>
> *(1) It would be useful to explain why the authors conducted their research using female rats but not male rats.*

Thank you for raising this insightful point. We chose female rats for the current study was based on several considerations. 1) Previous research has demonstrated that female rats exhibit metabolic dysfunction (e.g., hypertriglyceridemia, liver steatosis, insulin resistance) in response to dietary factors, such as high-sucrose feeding [16-19]. These metabolic characteristics made them an appropriate model for assessing the in vivo effects of JNK inhibition under high-sucrose conditions. 2) It is also reported that female rats show resilience to high-sucrose-induced metabolic dysfunction due to the protective effects of estrogen [8], we aimed to determine whether JNK inhibition could provide therapeutic benefits in this context. This allows us to evaluate the effect of JNK inhibition even in metabolically advantaged groups. 3) Our results from the tolerance test (Fig. 2a) indicated that female rats displayed more fluctuating variation to JNK-IN-5A administration. This variation allowed us to evaluate how JNK inhibition influences metabolic outcomes in a sex that is more responsive to the intervention. Nonetheless, we emphasize the importance of future studies involving male rats to better understand sex-specific responses to JNK inhibition and to provide more comprehensive guidance for the development of JNK-targeting therapies in MAFLD treatment.

> *(2) Figure 2C shows that JNK-IN-5A administration reduces the mRNA levels of Mapk8 and Mapk9 in the liver and the SkM. It would be useful to provide the authors' insight into the data.*

In the liver, the data in Fig. 2c in original submission and the attached Fig. 1 show that sucrose feeding induces opposite alterations in the mRNA expression of *Mapk8* (*Jnk1*, increased, $log2FC_{SucrosevsControl}$= 0.02) and *Mapk9* (*Jnk2*, decreased, $log2FC_{SucrosevsControl}$= -0.43), though these changes do not reach statistical significance. JNK-IN-5A administration reverses these effects, significantly decreasing *Mapk8* expression ($log2FC_{Sucrose+JNK\_D1vsSucrose}$= -0.37) while increasing *Mapk9* expression ($log2FC_{Sucrose+JNK\_D1vsSucrose}$= 0.42). This suggests potential differential yet compensatory roles of these two isoforms in regulating JNK activity during these interventions in the liver, keeping in line with the findings from *Jnk1*- and/or *Jnk2*-specific knockout studies [20, 21]. Additionally, emerging evidence indicates that *Jnk1* plays a major role in diet-induced liver fibrosis and metabolic dysfunction [22-25]. Therefore, the reduced *Mapk8* expression following JNK-IN-5A administration may contribute to the observed improvements in liver metabolism.

Author response image 1.

The spearman correlation between expression levels of *Mapk8*

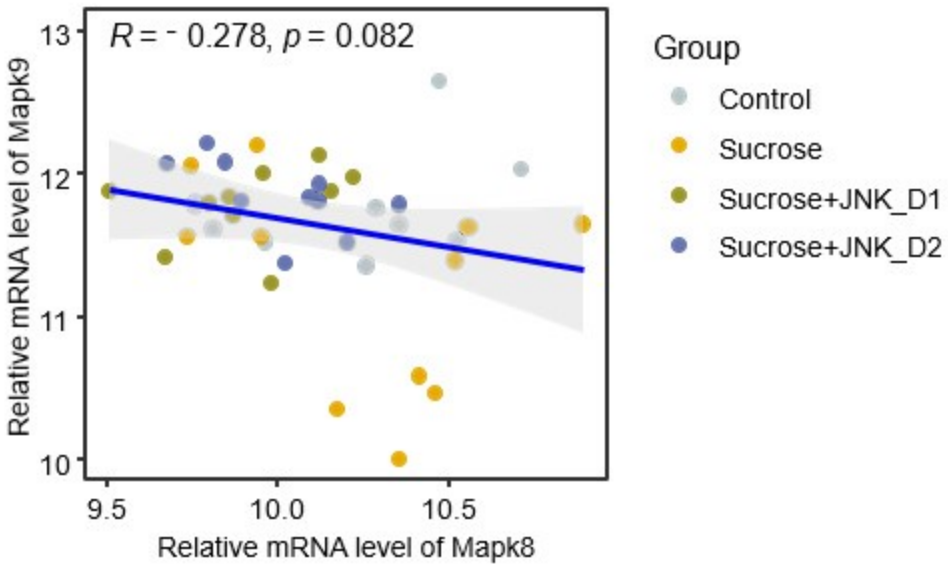

In skeletal muscle, the primary site for insulin-stimulated glucose uptake, insulin signaling is crucial for maintaining metabolic homeostasis [26]. Numerous studies have demonstrated that JNK activation promotes insulin resistance and targeting JNK might be a promising therapeutic strategy for the treatment of metabolic diseases associated with insulin resistance, such as MAFLD [24]. In our study, while sucrose overconsumption did not significantly alter the mRNA levels of JNK isoforms in this tissue, JNK-IN-5A at dosage 30 mg/kg/day administration significantly reduced the expression of both *Jnk1* and *Jnk2* as well as genes involved in insulin signaling (Fig. 5). This suggests a potential interplay between JNK inhibition and insulin signaling pathways in the skeletal muscle, where inhibition of JNK activity may improve insulin sensitivity by modulating these pathways. However, it is also crucial to investigate the longterm effects of JNK-IN-5A administration and its broader impact on many other physiological processes regulated by the JNK pathway. These aspects will be a focus of our future studies.

> *(3) The notations a and b in Figure S5 are missing.*

Thank you for this constructive comment. We have corrected this in the revised figure S5.

> *(4) Data S13 described in the figure legend for Figure 7 (lines 630 and 632) seems a mistake and should be Data S8.*
>
> *(5) The notations a, b, and c in Figure 7 are incorrect. The figure legend for Figure 7a doesn't seem to match the figure contents.*

We appreciate your attention to details regarding Fig. 7. We have corrected the reference and the figure legend in revised Fig. 7.

Reference

(1) Fujii, A., et al., *Sucrose Solution Ingestion Exacerbates DinitrofluorobenzeneInduced Allergic Contact Dermatitis in Rats.* Nutrients, 2024. 16(12).

(2) Sun, S., et al., *High sucrose diet-induced dysbiosis of gut microbiota promotes fatty liver and hyperlipidemia in rats.* J Nutr Biochem, 2021. 93: p. 108621.

(3) Qi, S., et al., *Inositol and taurine ameliorate abnormal liver lipid metabolism induced by high sucrose intake.* Food Bioscience, 2024. 60: p. 104368.

(4) Ramos-Romero, S., et al., *The Buckwheat Iminosugar d-Fagomine Attenuates Sucrose-Induced Steatosis and Hypertension in Rats.* Mol Nutr Food Res, 2020. 64(1): p. e1900564.

(5) Ortiz, S.R. and M.S. Field, *Sucrose Intake Elevates Erythritol in Plasma and Urine in Male Mice.* J Nutr, 2023. 153(7): p. 1889-1902.

(6) Beckmann, M., et al., *Changes in the human plasma and urinary metabolome associated with acute dietary exposure to sucrose and the identification of potential biomarkers of sucrose intake.* Mol Nutr Food Res, 2016. 60(2): p. 444-57.

(7) He, X., et al., *High Fat Diet and High Sucrose Intake Divergently Induce Dysregulation of Glucose Homeostasis through Distinct Gut Microbiota-Derived Bile Acid Metabolism in Mice.* J Agric Food Chem, 2024. 72(1): p. 230-244.

(8) Stephenson, E.J., et al., *Chronic intake of high dietary sucrose induces sexually dimorphic metabolic adaptations in mouse liver and adipose tissue.* Nat Commun, 2022. 13(1): p. 6062.

(9) Mock, K., et al., *High-fructose corn syrup-55 consumption alters hepatic lipid metabolism and promotes triglyceride accumulation.* J Nutr Biochem, 2017. 39: p. 32-39.

(10) Eryavuz Onmaz, D. and B. Ozturk, *Altered Kynurenine Pathway Metabolism in Rats Fed Added Sugars.* Genel Tıp Dergisi, 2022. 32(5): p. 525-529.

(11) Gariani, K., et al., *Eliciting the mitochondrial unfolded protein response by nicotinamide adenine dinucleotide repletion reverses fatty liver disease in mice.* Hepatology, 2016. 63(4): p. 1190-204.

(12) Togo, J., et al., *Impact of dietary sucrose on adiposity and glucose homeostasis in C57BL/6J mice depends on mode of ingestion: liquid or solid.* Mol Metab, 2019. 27: p. 22-32.

(13) Arifin, W.N. and W.M. Zahiruddin, *Sample Size Calculation in Animal Studies Using Resource Equation Approach.* Malays J Med Sci, 2017. 24(5): p. 101-105.

(14) Faul, F., et al., *G*Power 3: a flexible statistical power analysis program for the social, behavioral, and biomedical sciences.* Behav Res Methods, 2007. 39(2): p. 175-91.

(15) Bonapersona, V., et al., *Increasing the statistical power of animal experiments with historical control data.* Nat Neurosci, 2021. 24(4): p. 470-477.

(16) Kendig, M.D., et al., *Metabolic EYects of Access to Sucrose Drink in Female Rats and Transmission of Some EYects to Their OYspring.* PLoS One, 2015. 10(7): p. e0131107.

(17) Harris, R.B.S., *Source of dietary sucrose influences development of leptin resistance in male and female rats.* Am J Physiol Regul Integr Comp Physiol, 2018. 314(4): p. R598-R610.

(18) Velasco, M., et al., *Sexual dimorphism in insulin resistance in a metabolic syndrome rat model.* Endocr Connect, 2020. 9(9): p. 890-902.

(19) Maniam, J., C.P. Antoniadis, and M.J. Morris, *The eYect of early-life stress and chronic high-sucrose diet on metabolic outcomes in female rats.* Stress, 2015. 18(5): p. 524-37.

(20) Singh, R., et al., *DiYerential eYects of JNK1 and JNK2 inhibition on murine steatohepatitis and insulin resistance.* Hepatology, 2009. 49(1): p. 87-96.

(21) Sabapathy, K., et al., *Distinct roles for JNK1 and JNK2 in regulating JNK activity and c-Jun-dependent cell proliferation.* Mol Cell, 2004. 15(5): p. 713-25.

(22) Zhao, G., et al., *Jnk1 in murine hepatic stellate cells is a crucial mediator of liver fibrogenesis.* Gut, 2014. 63(7): p. 1159-72.

(23) Czaja, M.J., *JNK regulation of hepatic manifestations of the metabolic syndrome.* Trends Endocrinol Metab, 2010. 21(12): p. 707-13.

(24) Solinas, G. and B. Becattini, *JNK at the crossroad of obesity, insulin resistance, and cell stress response.* Mol Metab, 2017. 6(2): p. 174-184.

(25) Schattenberg, J.M., et al., *JNK1 but not JNK2 promotes the development of steatohepatitis in mice.* Hepatology, 2006. 43(1): p. 163-72.

(26) Sylow, L., et al., *The many actions of insulin in skeletal muscle, the paramount tissue determining glycemia.* Cell Metab, 2021. 33(4): p. 758-780.

https://doi.org/10.7554/eLife.98427.2.sa0